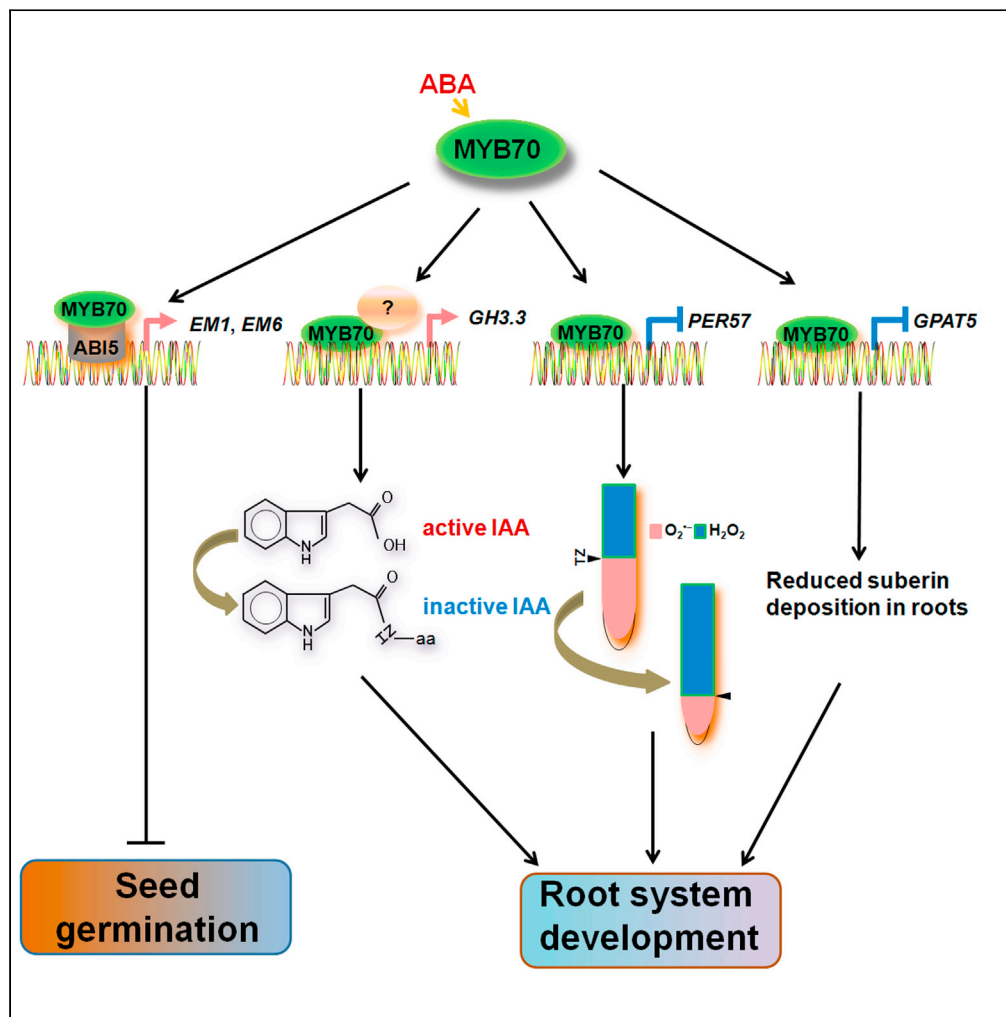**Article**

MYB70 modulates seed germination and root system development in *Arabidopsis*

Jinpeng Wan, Ruling Wang, Ping Zhang, ..., Shiyou Lü, Lam-Son Tran, Jin Xu

son.tran@ttu.edu (L.-S.T.)
xujin@sxau.edu.cn,
xujinsxau@163.com (J.X.)

Highlights

MYB70 regulates seed germination by enhancing ABA signaling via interaction with ABI5

MYB70 activates the IAA conjugation process by upregulating *GH3* genes expression

MYB70 mediates root growth via repression of *PER* genes

MYB70 negatively regulates suberin biosynthesis in roots

Article

MYB70 modulates seed germination and root system development in *Arabidopsis*

Jinpeng Wan,[1,6] Ruling Wang,[1] Ping Zhang,[1,2] Liangliang Sun,[1,2] Qiong Ju,[1,2] Haodong Huang,[5] Shiyou Lü,[5] Lam-Son Tran,[3,4,*] and Jin Xu[1,2,7,*]

SUMMARY

Crosstalk among ABA, auxin, and ROS plays critical roles in modulating seed germination, root growth, and suberization. However, the underlying molecular mechanisms remain largely elusive. Here, MYB70, a R2R3-MYB transcription factor was shown to be a key component of these processes in *Arabidopsis thaliana*. *myb70* seeds displayed decreased sensitivity, while MYB70-overexpressing *OX70* seeds showed increased sensitivity in germination in response to exogenous ABA through MYB70 physical interaction with ABI5 protein, leading to enhanced stabilization of ABI5. Furthermore, MYB70 modulates root system development (RSA) which is associated with increased conjugated IAA content and $H_2O_2/O_2^{\cdot-}$ ratio but reduced root suberin deposition, consequently affecting nutrient uptake. In support of these data, MYB70 positively regulates the expression of auxin conjugation-related *GH3*, while negatively peroxidase-encoding and suberin biosynthesis-related genes. Our findings collectively revealed a previously uncharacterized component that modulates ABA and auxin signaling pathways, $H_2O_2/O_2^{\cdot-}$ balance, and suberization, consequently regulating RSA and seed germination.

INTRODUCTION

Seed germination and root system architecture (RSA) are highly plastic in responses to environmental cues, and are fine-tuned by the crosstalk of different phytohormones and secondary signal molecules (Lata and Prasad, 2011; Lin et al., 2019; Signora et al., 2002). Abscisic acid (ABA) is a vital phytohormone, which plays key roles in modulating seed germination and various plant growth and developmental processes (Bu et al., 2009; Ding et al., 2015; Hirayama and Shinozaki, 2007; Zhang et al., 2019b). The basic leucine zipper (bZIP) transcription factor (TF), Abscisic Acid Insensitive 5 (ABI5), acts as a core regulator of the modulation of seed germination and seedling establishment (Finkelstein and Lynch, 2000). Many TFs or regulators modulate seed germination and seedling growth through regulation of *ABI5* expression, or physical interaction with ABI5 to alter ABI5's stabilization, or its regulatory effect on downstream target genes (Guan et al., 2014; Lim et al., 2013; Lopez-Molina et al., 2002; Zheng et al., 2012). For example, ABI3 modulates seed germination by directly inducing *ABI5* expression (Lopez-Molina et al., 2002). Meanwhile, ABI3 and DELLA proteins interact with ABI5 to form a complex and subsequently improve ABI5 capacity to induce the expression of high temperature-responsive genes, such as *SOMNUS* (*SOM*), which encodes a CCCH-type zinc finger protein that negatively regulates light-dependent seed germination in *Arabidopsis thaliana* to inhibit seed germination under high temperature conditions (Kim et al., 2008; Lim et al., 2013). The regulatory networks of seed germination and early seedling establishment involving ABA and associated TFs are extremely complex; and thus, a concerted effort is needed to identify and functionally characterize additional unknown members involved in these networks.

In *Arabidopsis*, early and quick auxin-responsive genes, including *Auxin/Indole-3-Acetic Acid* (*Aux/IAA*), *Gretchen Hagen3* (*GH3*), *Small Auxin-Up RNA* (*SAUR*), and *Auxin Response Factor* (*ARF*), are key performers in auxin signal transduction (Hagen and Guilfoyle, 2002; Kieffer et al., 2009; Tiwari et al., 2003; Vanneste and Friml, 2009). Auxin-induced *GH3* genes can mediate the inactivation of IAA by conjugation, which further attenuates auxin signal transduction (Staswick et al., 2005). Root system development is tightly modulated by various members of the auxin signaling (Vanneste and Friml, 2009). For example, auxin-inducible ARF7 and ARF19 regulate lateral root (LR) initiation and emergence by modulating the

[1]CAS Key Laboratory of Tropical Plant Resources and Sustainable Use, Xishuangbanna Tropical Botanical Garden, Chinese Academy of Sciences, Menglun, Mengla, Yunnan 666303, China

[2]College of Horticulture, Shanxi Agricultural University, Taigu 030801, China

[3]Institute of Research and Development, Duy Tan University, Da Nang 550000, Vietnam

[4]Institute of Genomics for Crop Abiotic Stress Tolerance, Department of Plant and Soil Science, Texas Tech University, Lubbock, TX 79409, USA

[5]State Key Laboratory of Biocatalysis and Enzyme Engineering, School of Life Sciences, Hubei University, Wuhan 430062, China

[6]Center of Economic Botany, Core Botanical Gardens, Chinese Academy of Sciences, Menglun, Mengla 666303, China

[7]Lead contact

*Correspondence:
son.tran@ttu.edu (L.-S.T.),
xujin@sxau.edu.cn,
xujinsxau@163.com (J.X.)
https://doi.org/10.1016/j.isci.2021.103228

expression of *Lateral Organ Boundaries Domain/Asymmetric Leaves 2-like* (*LBD/ASL*) genes *LBD18/ASL20*, *LBD16/ASL18* and *LBD29/ASL16* (Lee et al., 2009; Okushima et al., 2007).

Reactive oxygen species (ROS), as a secondary signaling molecule, play critical roles in modulating different developmental processes (Manzano et al., 2014). ROS are majorly generated in chloroplasts, mitochondria, peroxisomes, and the apoplast (Mittler et al., 2011; Vaahtera et al., 2014). Intracellular ROS equilibrium is fine-tuned by a series of reactions involving a set of enzymes, including NADPH/NADH oxidases, and antioxidant enzymes like catalases, peroxidases (PERs) and superoxide dismutases (Hossain et al., 2015; Mostofa et al., 2018). Many studies have shown that ROS are responsible for the alteration of RSA (Manzano et al., 2014; Tsukagoshi et al., 2010). The basic-helix-loop-helix (bHLH) Upbeat1 (UPB1) TF modulates the balance between differentiation and proliferation in the roots by regulating ROS levels via direct repression of several *PER* genes, thereby modulating root growth and development (Tsukagoshi et al., 2010). In addition to UPB1, MYB36 also showed a similar function in regulating lateral root primordium (LRP) development and ROS balance in *Arabidopsis* roots by modulating the transcription of a set of *PER* genes (Fernández-Marcos et al., 2017). Nevertheless, Mabuchi et al. (2018) found that MYB30 regulates primary root (PR) growth in an H_2O_2-dependent manner.

Cutin and suberin, the two types of lipid polyesters, act as transport barriers at the interface between plants and the environment (Holbein et al., 2021; Schreiber, 2010). Recent studies have shown the important roles of cuticle and suberin in modulating seed and root development (Barberon et al., 2016; Beisson et al., 2007; Coen et al., 2019). The Glycerol-3-Phosphate Acyltransferase 5 (GPAT5) positively regulates suberin biosynthesis in seed coats and roots (Beisson et al., 2007), while GPAT4 and GPAT8 functionally and redundantly regulate cuticle formation in root cap, and hence affect LR formation (Berhin et al., 2019). Several MYB TFs modulate the expression of genes involved in cuticle and suberin biosyntheses in plants. For example, in *Arabidopsis*, MYB96 positively regulates cuticular wax biosynthesis in an ABA-dependent manner (Seo et al., 2009), while MYB9 and MYB107 are responsible for suberin deposition in seed coats (Lashbrooke et al., 2016).

The *Arabidopsis MYB44*, *MYB70*, *MYB73*, and *MYB77* genes, which share structural similarity and are the members of subfamily 22, are involved primarily in the regulation of plant growth and development, as well as plant responses to environmental stresses (Jung et al., 2008; Yang et al., 2019). MYB77 modulates LR growth and development through auxin signaling pathway by physically interacting with ARF7 (Shin et al., 2007; Zhao et al., 2014). The ABA receptor Pyrabactin Resistance 1-Like 8 (PYL8) mediates LR growth by physically interacting with and enhancing the activity of MYB77, as well as its homologs MYB44 and MYB73, to activate auxin signaling (Zhao et al., 2014). However, the functions of MYB70 in mediating plant growth and development have not yet been elucidated.

Here, we focused on characterizing the mechanisms of MYB70 involved in the processes of seed germination and root system development through the modulation of its dual transcriptional regulatory activities. *myb70* seeds displayed decreased sensitivity, while MYB70-overexpressing *OX70* seeds showed increased sensitivity in germination in response to exogenous ABA. We then used yeast two-hybrid (Y2H) assay to search for MYB70-interacting proteins or transcriptional regulators and identified the basic region/leucine zipper TF ABI5. Our results indicated that MYB70 is an important TF involved in ABI5-mediated seed germination. MYB70 also regulates root system growth and development by altering auxin signaling via its transactivation activity, while controlling ROS equilibrium via its transcriptional repression activity. MYB70 negatively regulates suberin deposition in the roots to modulate RSA via its transcriptional repression activity. Overall, our study showed that MYB70 integrates auxin, ROS and ABA signaling pathways to form a network regulating seed germination and root system development. These results enables us to gain further understanding on how MYB TFs may contribute to improving the roots' ability in nutrient and water uptake to maintain normal plant growth in an era of climate change.

RESULTS

Determination of the developmental and tissue-specific expression of *MYB70*

The expression of the *MYB70* gene was localized using a transgenic line in which *β-glucuronidase* (*GUS*) was fused to the 1.5-kb promoter region of *MYB70*. GUS activity was found in the micropyle region of seeds (Figure 1Aa), in the radicles (Figure 1Ab), and in the cotyledons (Figures 1Ab, 1Ac and 1Af). In addition, GUS activity was detected in the entire roots (Figures 1Ac–1Ae) and young leaves (Figure 1Af). In mature plants,
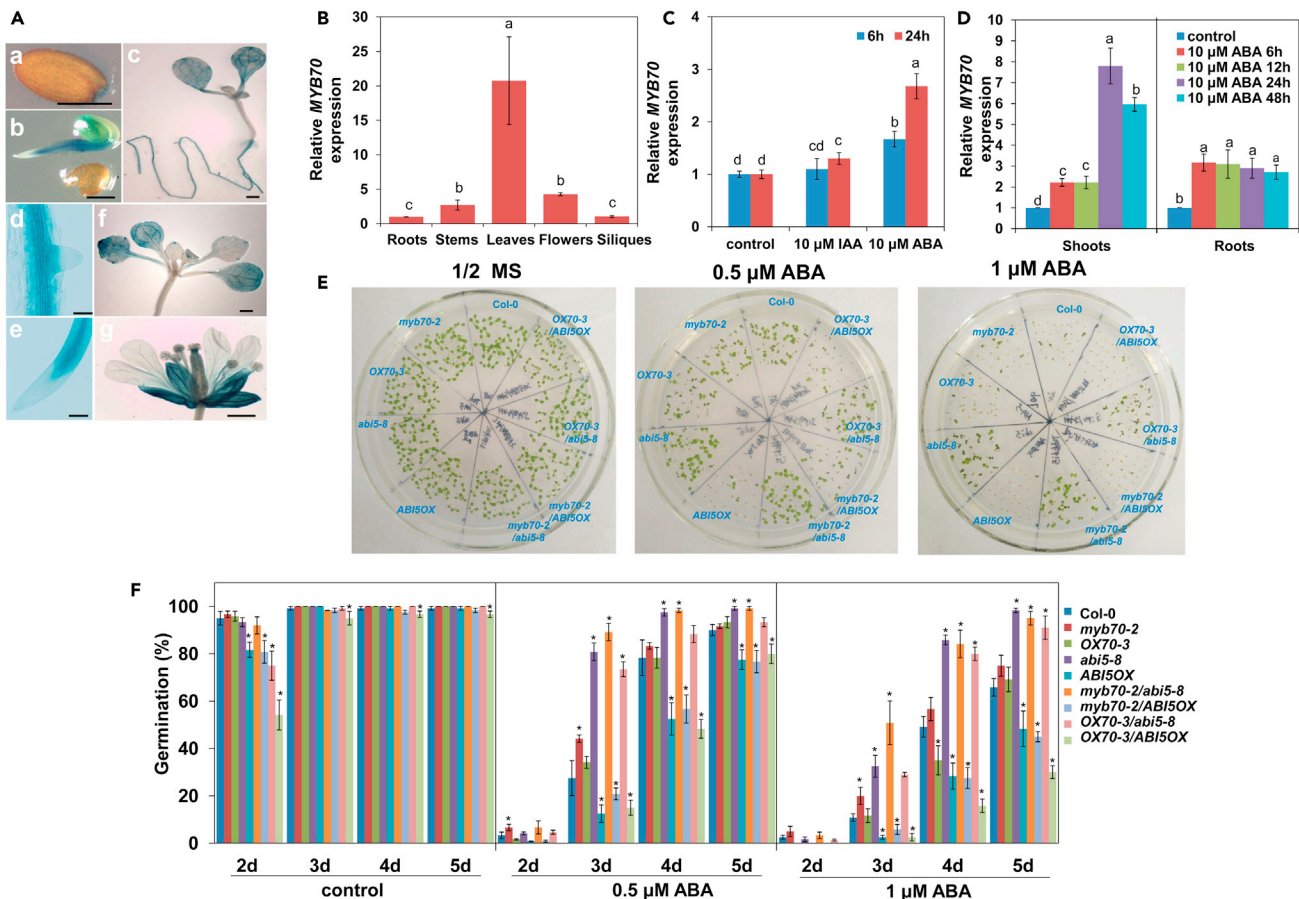
Figure 1. The gene expression analysis of _MYB70_ and seed germination in response to exogenous ABA in _myb70_ and _abi5_ mutants, _ABI5_-overexpressing _ABI5OX_ and _MYB70_-overexpressing _OX70_ transgenic plants, and their different combinations

(A) Detection of _MYB70_ expression using the _proMYB70:GUS_ transgenic line. GUS staining observed in seeds (bar, 500 μm) (a), 1-day-old seedling (bar, 500 μm) (b), 7-day-old seedling (bar, 500 μm) (c), lateral root (bar, 100 μm) (d), root tip of primary root (bar, 100 μm) (e), leaves of 15-day-old seedling (bar, 500 μm) (f) and flowers (bar, 500 μm) (g).

(B) Relative expression of the _MYB70_ gene in Col-0 plants.

(C) Relative expression of the _MYB70_ gene in 5-day-old Col-0 seedlings with or without 10 μM IAA or 10 μM ABA for 6 or 24 h.

(D) Relative expression of the _MYB70_ gene in the shoots or roots of 5-day-old Col-0 seedlings with or without 10 μM ABA for 6, 12, 24 and 48 h. Results shown are means ± SD ($n = 3$).

(E) Seeds of _abi5_ and _myb70_ mutants, and _ABI5_-overexpressing _ABI5OX_ and _MYB70_-overexpressing _OX70_ transgenic plants, and their different combinations after stratification at 4°C for 2 days were germinated on 1/2-strength MS medium with or without 0.5 μM or 1 μM abscisic acid (ABA) for an additional 7 days.

(F) Seed germination was determined 2–5 days after stratification on 1/2-strength MS medium without or with 0.5 μM ABA or 1 μM ABA. Results are means ± standard error (SEM) ($n = 5$, more than 120 seeds/genotype/repeat). Different letters show significantly different values at $p < 0.05$ according to a Tukey's test, and asterisks show significant differences from the control (Student's _t_-test, $p < 0.05$).

GUS activity was also detected in the flowers and siliques (Figure 1Ag). Additionally, _MYB70_ expression patterns were also examined in different tissues using qRT-PCR (Figure 1B).

Since both auxin and ABA play important roles in modulating plant growth and development (Zhao et al., 2014), we also examined _MYB70_ expression in response to exogenous IAA and ABA treatments. The expression of _MYB70_ might be slightly induced and markedly upregulated in the whole seedlings in response to exogenous IAA and ABA, respectively, after 24 h of treatment (Figure 1C). When the expression patterns of _MYB70_ in response to exogenous ABA were studied separately in shoots and roots, the _MYB70_ transcription was more highly induced by ABA in shoots than in roots (Figure 1D). Additionally, the expression of _MYB70_ reached the highest levels in the roots and shoots after 6 and 24 h of treatment, respectively, after which its expression levels gradually declined (Figure 1D).

MYB70 negatively regulates seed germination in an ABA-dependent manner by physically interacting with ABI5

We obtained two T-DNA insertion mutants, *myb70-1* and *myb70-2*, from the European Arabidopsis Stock Centre (NASC), and also developed *35S:MYB70* (*OX70-1*, *OX70-2*, *OX70-3*, *OX70-4*, *OX70-5* and *OX70-6*) transgenic *Arabidopsis* lines for *in planta* functional analysis of MYB70. Quantitative reverse transcription-polymerase chain reaction (qRT-PCR)-based analysis revealed that *MYB70* expression was highly up-regulated in *OX70* plants but was abolished in the two mutants (Figures S1A and S1B).

ABA plays an essential role in modulating seed germination (Guan et al., 2014). The expression of *MYB70* was markedly induced by ABA (Figures 1C and 1D). We, thus, germinated seeds of *OX70*, *myb70* and Col-0 plants on 1/2-strength Murashige and Skoog (MS) medium supplied with or without ABA to investigate the possible role of MYB70 in seed germination. When compared with Col-0 seeds in a seed germination assay as assessed by seed radicle appearance, *myb70* seeds displayed decreased sensitivity, while *OX70* seeds exhibited increased sensitivity to ABA (Figures 1E and 1F). The result suggested that MYB70 negatively regulates seed germination in an ABA-dependent manner.

We then searched for MYB70-interacting proteins to identify potential regulators/coregulators, particularly those involved in ABA-mediated regulation of seed germination. Among the potential MYB70-interacting proteins, the B-group ABI protein, ABI5, which plays a vital role in modulating seed germination (Zhao et al., 2018; Zhou et al., 2015), was identified. We then performed a Y2H assay using ABI5 (fused to the binding domain of GAL4; BD-ABI5) as bait and MYB70 (fused to the activation domain of GAL4; AD-MYB70) as prey. The result of the Y2H assay showed that ABI5 indeed interacted with MYB70 in the yeast cells (Figure 2A). This interaction was also verified by an *in vitro* pull-down assay. As shown in Figure 2B, glutathione *S*-transferase (GST)-fused ABI5 could retain MYB70-His, while GST alone could not. This physical interaction was also corroborated by the results of a coimmunoprecipitation (Co-IP) assay (Figure 2C). We further analyzed the interaction between the two proteins in plant cells using the bimolecular fluorescence complementation (BiFC) assay, in which the MYB70 and ABI5 proteins were fused to the N-terminal part and the C-terminal part of the yellow fluorescent protein (YFP), respectively. A strong YFP fluorescence signal was detected in the nuclei, when ABI5 and MYB70 fusions were examined together (Figure 2D). Taken together, these data indicated that ABI5 interacts with MYB70 both *in vivo* and *in vitro*.

We then compared the expression of *MYB70* and *ABI5* in both dry and germinating seeds. The expression patterns of *MYB70* were similar to those of *ABI5* in both types of seeds (Figures 2E and 2F). These data collectively suggested that MYB70 may play a role in seed germination, perhaps through interaction with ABI5. To elucidate the potential genetic interaction of MYB70 and ABI5 in the mediation of ABA-induced repression of seed germination, we generated hybrid *OX70 ABI5OX*, *OX70 abi5*, *myb70 ABI5OX*, and *myb70 abi5* lines by crossing *ABI5OX* or *abi5-8* (SALK_013163) with *OX70* or *myb70* lines. We then evaluated seed germination rates of *ABI5OX*, *abi5-8*, *OX70*, *myb70*, *OX70 ABI5OX*, *myb70 ABI5OX*, *myb70 abi5* and *OX70 abi5* genotypes in response to ABA. The seeds of *ABI5OX* were highly sensitive to ABA during germination, whereas those of *abi5-8* were highly insensitive to ABA (Figure 1). Similar to the seeds of *ABI5OX* plants, the seeds of hybrid *OX70 ABI5OX* (Figure S2) and *myb70 ABI5OX* lines were hypersensitive, and similar to those of the *abi5-8* mutants, the seeds of hybrid *OX70 abi5* and *myb70 abi5* lines were insensitive to ABA during germination (Figures 1E and 1F). These results indicated that MYB70 functions as a negative regulator of seed germination by acting together with ABI5 in modulation of ABA signaling where ABI5 plays a more prominent role.

To confirm these results, we evaluated the expression of *EM1* and *EM6* genes, each of which is a direct target of ABI5, in the germinating seeds of the double mutants. The transcript levels of both the *EM1* and *EM6* genes were higher in the hybrid *OX70 ABI5OX* and *myb70 ABI5OX* lines than in the Col-0 and *myb70* mutant plants, while their transcript levels were similar in the *abi5-8*, *OX70 abi5*, and *myb70 abi5* lines (Figures 3A and 3B). We also measured ABA levels in the *OX70* plants and *myb70* mutants, and found no difference between these lines (Figure 3C). These data demonstrated that MYB70 was involved in regulating ABA-mediated seed germination by enhancing ABA signaling via interaction with ABI5, but not by increasing the ABA content.

We next investigated the role of the MYB70-ABI5 interaction on the transcriptional regulation of the *EM1* and *EM6* genes that are the direct targets of ABI5 (Finkelstein and Lynch, 2000). *35S:ABI5* was cotransfected with *35S:MYB70* together with *EM1-LUC* or *EM6-LUC* reporter plasmids. Overexpression of *ABI5* or *MYB70*
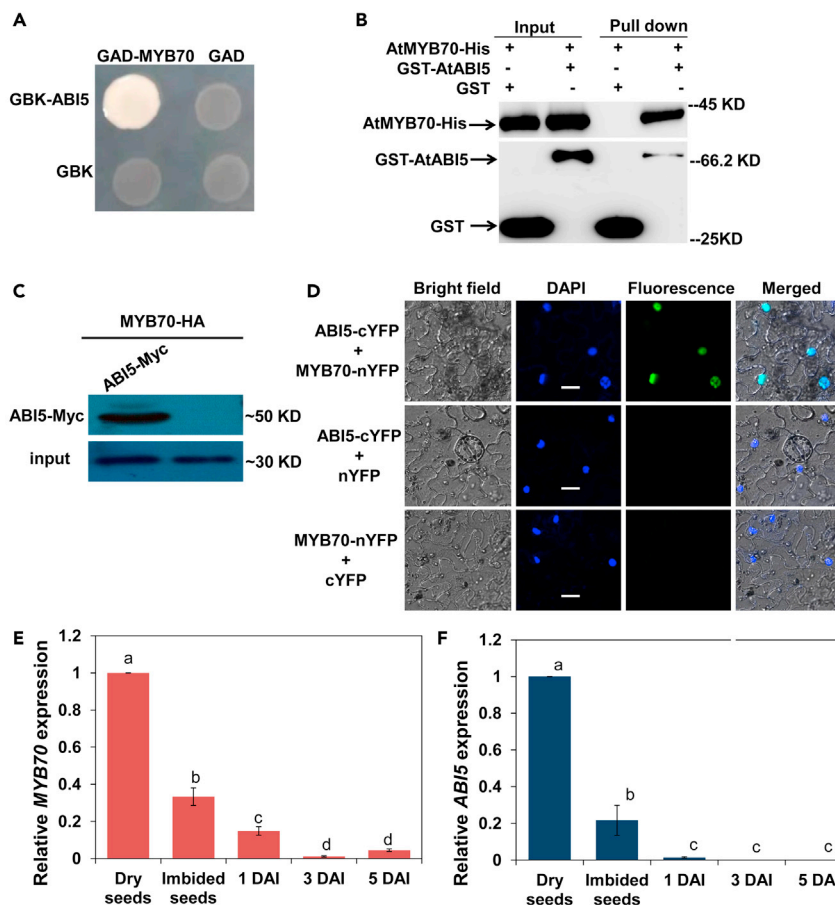
Figure 2. MYB70 interacts with ABI5 both *in vitro* and *in vivo*

(A) Yeast-two-hybrid (Y2H) analysis revealed an interaction between MYB70 and ABI5. Transformed yeast cells were grown on SD-Trp/-His/-Leu/-Ade medium.

(B) *In vitro* pull-down assay revealed the interaction between MYB70 and ABI5.

(C) Coimmunoprecipitation assay showing the interaction between MYB70 and ABI5.

(D) BiFC analysis of the interaction between MYB70 and ABI5. DAPI, 4',6-diamidino-2-phenylindole. Fluorescence that was resulted from complementation of the N-terminal region of YFP fused to MYB70 (MYB70-nYFP) with the C-terminal region of YFP fused to ABI5 (ABI5-cYFP) was observed in the nuclei of *N. benthamiana* leaves. No signal was observed in the negative controls. The blue and green fluorescence represent DAPI and GFP, respectively (bar, 50 μm).
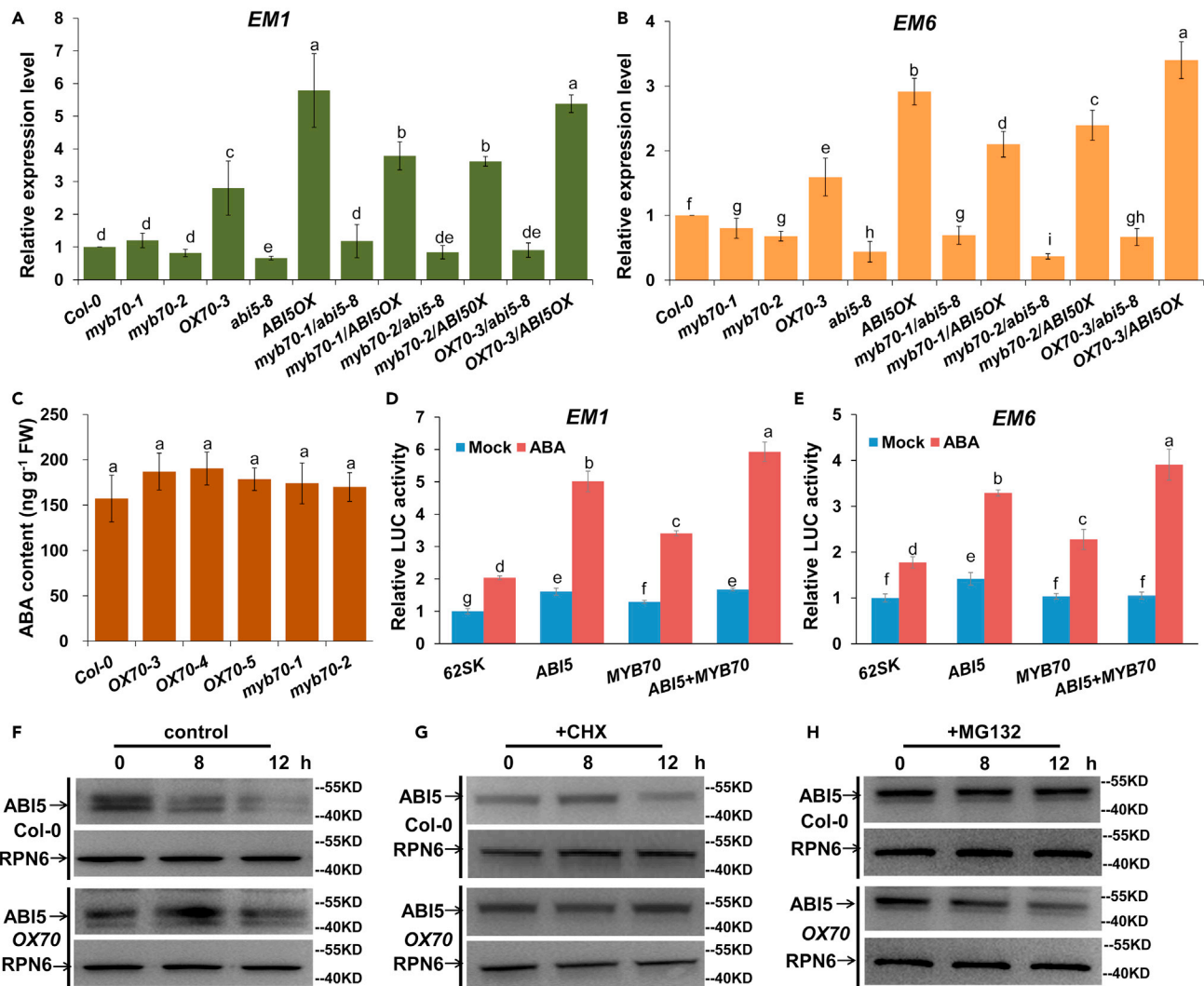
(E and F) Relative expression of *MYB70* (E) and *ABI5* (F) in dry and germinating Col-0 seeds at different stages. The expression level of *MYB70* and *ABI5* in the dry Col-0 seeds was set to 1. Results shown are means $\pm$ SD ($n = 3$, more than 120 seeds/genotype/repeat). Different letters show significantly different values at $p < 0.05$ according to a Tukey's test.

increased the expression of the *EM1* and *EM6* genes, especially in the presence of ABA, with overexpression of *ABI5* showing higher effect than that of *MYB70* (Figures 3D and 3E). Cotransfection of *35S:ABI5* and *35S:MYB70* constructs stimulated *EM1* and *EM6* expression more than that of any single construct (Figures 3D and 3E), suggesting that the interaction of ABI5 with MYB70 improved ABI5's ability to transcriptionally regulate its target genes.

MYB70 interaction with ABI5 prevents ABI5 from 26S proteasome-dependent degradation

Previous studies have demonstrated that ABA stabilized ABI5 protein, since ABI5 was degraded via 26S proteasome in the absence of exogenous ABA (Lopez-Molina et al., 2002; Seo et al., 2014). To determine whether MYB70 regulates ABI5 stabilization, the ABA-treated Col-0 and *OX70* seeds were transferred to fresh 1/2 MS liquid medium without ABA for 8 and 12 h. As shown in Figure 3F, ABI5 was more abundant in *OX70* seeds in the absence of ABA. After treatment with protein synthesis inhibitor cycloheximide (CHX), ABI5 degradation was also delayed in *OX70* compared with Col-0 seeds (Figure 3G). However, treatment

Figure 3. Interaction between MYB70 and ABI5

(A and B) Relative expression of the *EM1* and *EM6* genes in the *myb70 abi5* double mutant and other related mutants and transgenic lines. The expression levels of the *EM1* and *EM6* genes in Col-0 were set to 1. Results shown are means $\pm$ SD ($n = 3$).

(C) ABA contents in *myb70* mutant and *MYB70*-overexpressing *OX70* transgenic plants. Results shown are means $\pm$ SD ($n = 3$, more than 260 seeds/genotype/repeat).

(D and E) Transient dual-LUC reporter assays indicated activation of *EM1* and *EM6* gene expression by *MYB70*, *ABI5* or their combination in the presence or absence of 5 μM ABA. 62SK, *ABI5* and *MYB70* represent the empty pGreenII 62-SK, pGreenII 62-SK-ABI5 and pGreenII 62-SK-MYB70 vectors, respectively. *EM1* and *EM6* represent pGreenII 0800-pEM1::LUC and pGreenII 0800-pEM6::LUC, respectively. Results shown are means $\pm$ SD ($n = 3$). Different letters show significantly different values at $p< 0.05$ according to a Tukey's test.

(F–H) MYB70 stabilized ABI5 protein. Seeds of Col-0 and *OX70* plants were treated with 5 μM ABA in white light for 3 days and then harvested at 0, 8 and 12 h after the removal of ABA by either being washed out with liquid medium (F), after treatment with the protein synthesis inhibitor CHX (100 μM) (G), or after the proteasome inhibitor MG132 (50 μM) (H). RPN6, loading control. The experiments were repeated three times with similar results.

with proteasome inhibitor MG132 delayed ABI5 degradation in both Col-0 and *OX70* seeds, indicating that ABI5 degradation was 26S proteasome-dependent (Figure 3H). Taken together, these results indicated that the higher abundance of ABI5 in *OX70* was resulted from the reduced degradation of ABI5 due to the function of MYB70.

MYB70 modulates root system architecture

We analyzed the role of *MYB70* in regulating RSA. As shown in Figures 4A and 4B, the PRs of the *OX70* lines (e.g. *OX70-3*, *OX70-4* and *OX70-5*) were shorter than those of Col-0, while the PRs of *myb70* mutant and
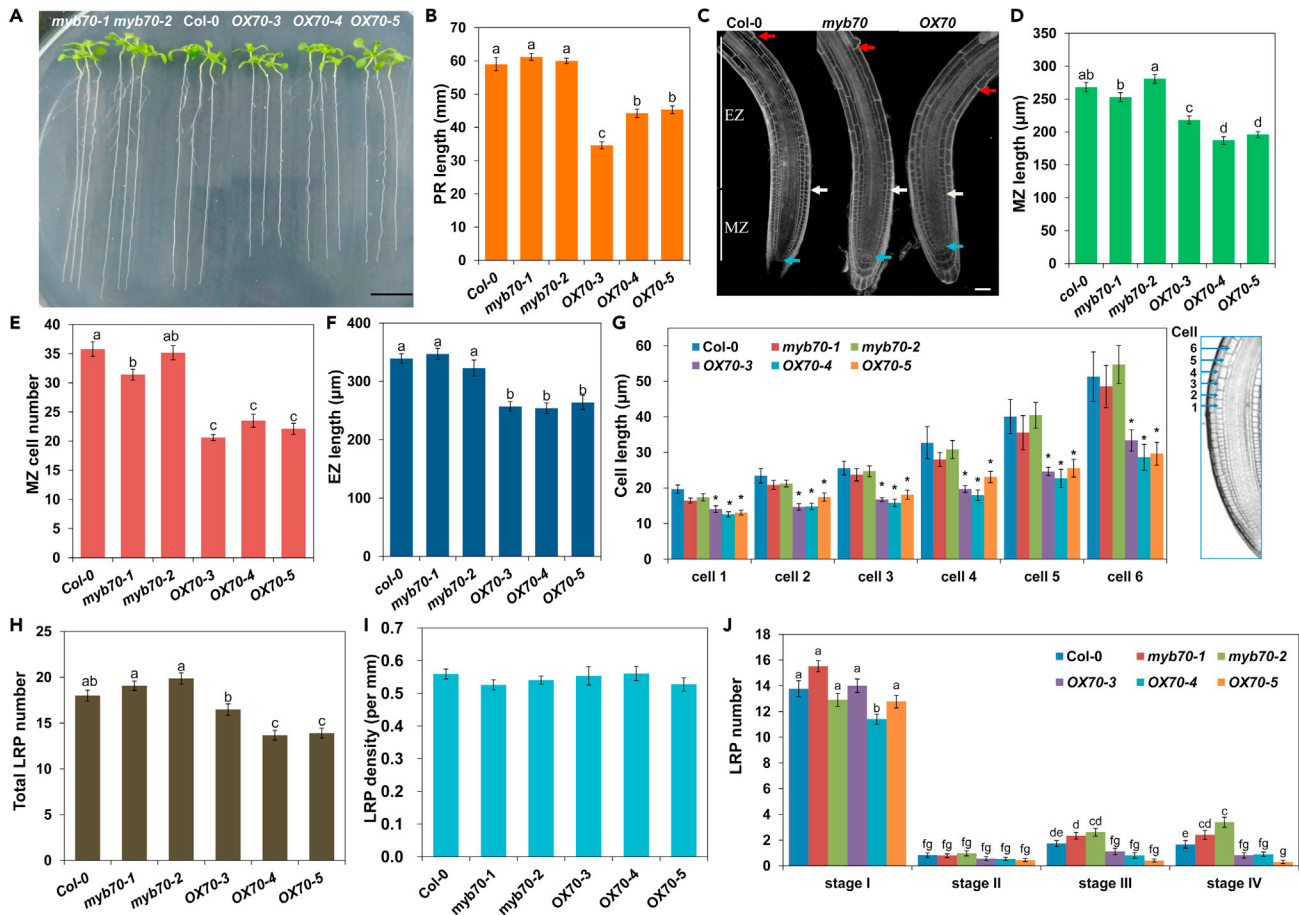
**Figure 4. Root phenotypes of *myb70* mutant lines and *MYB70*-overexpressing *OX70* transgenic plants**
(A) Col-0, *myb70* mutant and *OX70* seedlings grown in 1/2-strength MS medium for 9 days (bar, 1 cm).
(B–J) Primary root (PR) length (B), meristematic zone (MZ) length (C, D), MZ cell number (E), elongation zone (EZ) length (C, F), the cell length of six consecutive cells in the transition zone (G), total lateral root primordium (LRP) number (H), LRP density (I) and LRP number (J) were measured. Results are means ± standard error (SEM) (*n* = 3, more than 20 plants/genotype/repeat). Different letters show significantly different values at *p*< 0.05 according to a Tukey's test.

Col-0 plants showed no obvious phenotypic differences. To investigate the role of *MYB70* in PR growth in more detail, we measured the length of the meristematic zone (MZ) and the elongation zone (EZ), MZ cell number and the length of six consecutive cells in the transition zone. Both the MZ and EZ were significantly shorter (Figures 4C–4F), and the cells in the transition zone were more slowly elongated (Figure 4G) in *OX70* transgenic plants than those in the Col-0 plants and the *myb70-1* and *myb70-2* mutants. To further explore the role of *MYB70* on LR growth and development, we investigated the LRP initiation. The total number of LRPs was reduced; however, the LRP density was unaffected by overexpression of *MYB70* (Figures 4H and 4I). Investigation of the four stages of LRPs indicated that overexpression of *MYB70* reduced the number of LRPs in stages III and IV (Figure 4J). Taken together, these data indicated that *MYB70* regulates RSA by affecting both PR growth and LR formation, perhaps in a negative manner.

MYB70 plays a role in root system development by altering the auxin response by increasing the conjugated IAA level

Next, we were interested in whether the reduced PR growth and LR formation observed in the *OX70* lines occurred in an auxin-dependent manner. To address this question, we first investigated the effects of exogenous IAA on the root growth of the *OX70*, *myb70* and Col-0 plants. Exogenous IAA inhibited PR growth and induced LR formation; however, overexpression of *MYB70* resulted in reduced sensitivity to IAA, especially at high IAA concentrations (Figures 5A–5D). Specifically, in the presence of 75 nM IAA, the decrease
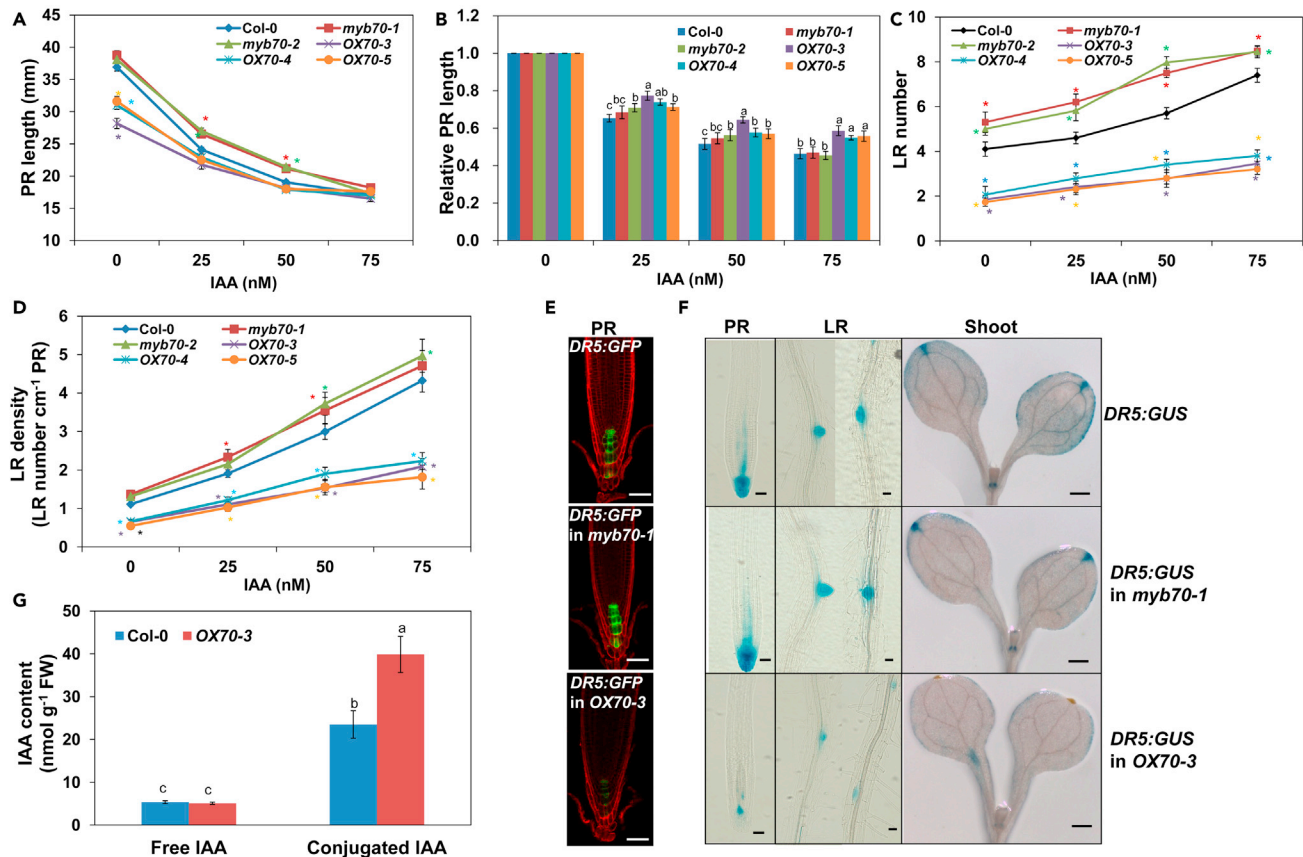
Figure 5. Overexpression of *MYB70* modulates root system growth by reducing the auxin response by increasing the conjugated IAA level

(A–D) Five-day-old Col-0, *myb70* mutant and *MYB70*-overexpressing *OX70* seedlings germinated on 1/2-strength MS medium were transplanted onto fresh medium supplemented with 0, 25, 50 or 75 nM indole-3-acetic acid (IAA) for 5 days, after which the primary root (PR) length (A), relative PR length (B), lateral root (LR) number (C) and LR density (D) were measured. Results are means $\pm$ standard error (SEM) ($n = 3$, more than 20 seeds/genotype/repeat).

(E) Expression of *DR5:GFP* in the root tips of Col-0, *myb70* mutant and *OX70* seedlings (bar, 50 μm).

(F) Expression of *DR5:GUS* in the PRs (bar, 50 μm), LRs (bar, 50 μm) and shoots (bar, 500 μm) of Col-0, *myb70* mutant and *OX70* seedlings.

(G) Free and conjugated indole-3-acetic acid (IAA) levels in Col-0 and *OX70* seedlings. Results are means $\pm$ standard error (SEM) ($n = 3$, more than 200 seeds/genotype/repeat). Different letters show significantly different values at $p < 0.05$ according to a Tukey's test, and the asterisks show significant differences from the control (Student's t-test, $p < 0.05$).

rates of PR length of *OX70-3*, *OX70-4* and *OX70-5* seedlings were 12.9%, 8.8% and 9.7%, respectively, lower than that of Col-0 (Figure 5B), while the increase rates of LR density of *OX70-3*, *OX70-4* and *OX70-5* seedlings were 69.5%, 53.5% and 57.5%, respectively, lesser than that of Col-0 (Figure 5D). Taken together, these data indicated that MYB70, at least in part, altered root growth by repressing the responsiveness to auxin.

To elucidate whether and how MYB70 affects auxin signaling, *OX70* and *myb70* lines were crossed with *DR5:GUS* and *DR5:GFP* reporter plants, respectively. Compared with the *DR5:GFP* and *myb70/DR5:GFP* seedlings, the *OX70/DR5:GFP* seedlings presented remarkably decreased GFP fluorescence in the root tips when grown in 1/2-strength MS medium (Figure 5E). Similarly, compared with the *DR5:GUS* and *myb70/DR5:GUS* seedlings, the *OX70/DR5:GUS* seedlings showed clearly decreased GUS activities in the root tips of PRs, LRs and cotyledons when they were grown in 1/2-strength MS medium (Figure 5F). To verify these observations, we compared the free and conjugated IAA concentrations in the *OX70* and Col-0 seedlings. There was no significant difference in the free IAA concentration between the *OX70* and Col-0 plants; however, the *OX70* plants showed 69.4% higher conjugated IAA concentration relative to that of the Col-0 plants (Figure 5G). These results collectively suggested that MYB70 affects auxin signaling by converting active IAA into inactive conjugated IAA.

Comparative transcriptome analysis revealed molecular functions of MYB70 during root system development

To gain molecular insights into how MYB70 modulates RSA, we carried out a transcriptome analysis of *OX70*, *myb70*, and Col-0 plants using RNA-sequencing (RNA-seq) with three biological repeats. 974 DEGs were identified from the *OX70*/WT comparison (621 upregulated and 353 downregulated genes), while 237 DEGs were found from the *myb70*/WT comparison (208 upregulated and 29 downregulated genes) ($\log_2$ fold change ≥ 1 or ≤ -1; $q \leq 0.001$) (Figure S3; Data S1 and S2).

We then performed a Gene Ontology (GO) enrichment analysis to investigate the molecular mechanisms underlying MYB70-mediated growth and development. 'Peroxidase activity', 'Oxidoreductase activity, acting on peroxide as acceptor' and 'Antioxidant activity' were among the significantly TOP20 enriched pathways of *OX70*-downregulated genes (Figure S4A). We then performed Kyoto Encyclopedia of Genes and Genomes (KEGG) pathway analysis according to the DEG results, *OX70*-downregulated 17%, 27%, and 4% of DEGs were enriched in 'Phenylpropanoid biosynthesis', 'Biosynthesis of secondary metabolites' and 'cutin, suberin, and wax biosynthesis', respectively (Figure S4B). These results suggested that MYB70 may modulate the ROS metabolic process and suberin biosynthesis.

MYB70 activates the auxin conjugation process by directly upregulating the expression of *GH3* genes during root system development

The above results indicated that overexpression of *MYB70* increased the levels of conjugated IAA (Figure 5G), and upregulated the expression of several auxin-responsive genes, including *GH3.3* and *GH3.5*, in the *OX70* compared with Col-0 plants (Figure S5). *GH3* genes encode IAA-conjugating enzymes that inactivate IAA (Park et al., 2007). *MYB70* expression was markedly induced by ABA and slightly induced by IAA (Figure 1C); thus, we examined the effects of ABA and IAA on the expression of *GH3* genes in *OX70*, *myb70*, and Col-0 plants. Exogenous ABA or IAA induced the expression of *GH3.1*, *GH3.3*, and *GH3.5* both in roots and whole seedlings, with higher expression levels being observed in *OX70* than Col-0 and *myb70* plants (Figures 6A–6F, and S6A). These results indicated that MYB70-mediated auxin signaling was, at least in part, integrated into the ABA signaling pathway and that *GH3* genes were involved in this process.

To investigate whether MYB70 could directly regulate the transcription of *GH3* genes, we selected *GH3.3*, which can modulate root system development by increasing inactive conjugated IAA levels (Gutierrez et al., 2012), as a representative gene for a yeast-one-hybrid (Y1H) assay to examine the binding of MYB70 to its promoter, and found that MYB70 could bind to the tested promoter region (Figure S7). We then performed an electrophoretic mobility shift assay (EMSA) to test for possible physical interaction between MYB70 and the promoter sequence. Two R2R3-MYB TF-binding motifs, the MYB core sequence 'YNGTTR' and the AC element 'ACCWAMY', have been discovered in the promoter regions of MYB target genes (Kelemen et al., 2015). Analysis of the promoter of *GH3.3* revealed several MYB-binding sites harboring AC element and MYB core sequences. We chose a 34-bp region containing two adjacent MYB core sequences (TAGTTTTAGTTA) in the approximately −1,534- to −1501-bp upstream of the starting codon in the promoter region. EMSA revealed that MYB70 interacted with the fragment, but the interaction was prevented when unlabeled cold probe was added, indicating the specificity of the interaction (Figure 6G). To further confirm these results, we performed chromatin immunoprecipitation (ChIP)-qPCR against the *GH3.3* gene using the *35S:MYB70-GFP* transgenic plants. The transgenic plants showed an altered phenotype (different PR length and LR numbers), which was similar to that of the *OX70* lines, demonstrating that the MYB70-GFP fusion protein retained its biological function (Figure S8). We subsequently designed three pairs of primers that contained the MYB core sequences for the ChIP-qPCR assays. As shown in Figure 6H, significant enrichment of MYB70-GFP-bound DNA fragments was observed in the three regions of the promoter of *GH3.3*.

To further confirm that MYB70 transcriptionally activated the expression of *GH3.3*, we cotransfected the 35S:MYB70 (pGreen II 62-SK-MYB70) plasmid along with the *GH3.3-LUC* (pGreen II 0800-promoterGH3.3-Luciferase) reporter construct. Cotransfection of MYB70 increased *GH3.3* expression, especially under IAA treatment (Figure 6I), supporting the results of transcriptome and qRT-PCR analyses and indicated that MYB70 directly binds to the promoter of *GH3.3* gene and upregulates its transcription. These results collectively suggested MYB70 modulates root system development by directly activating the auxin conjugation process through upregulating the expression of *GH3* genes.
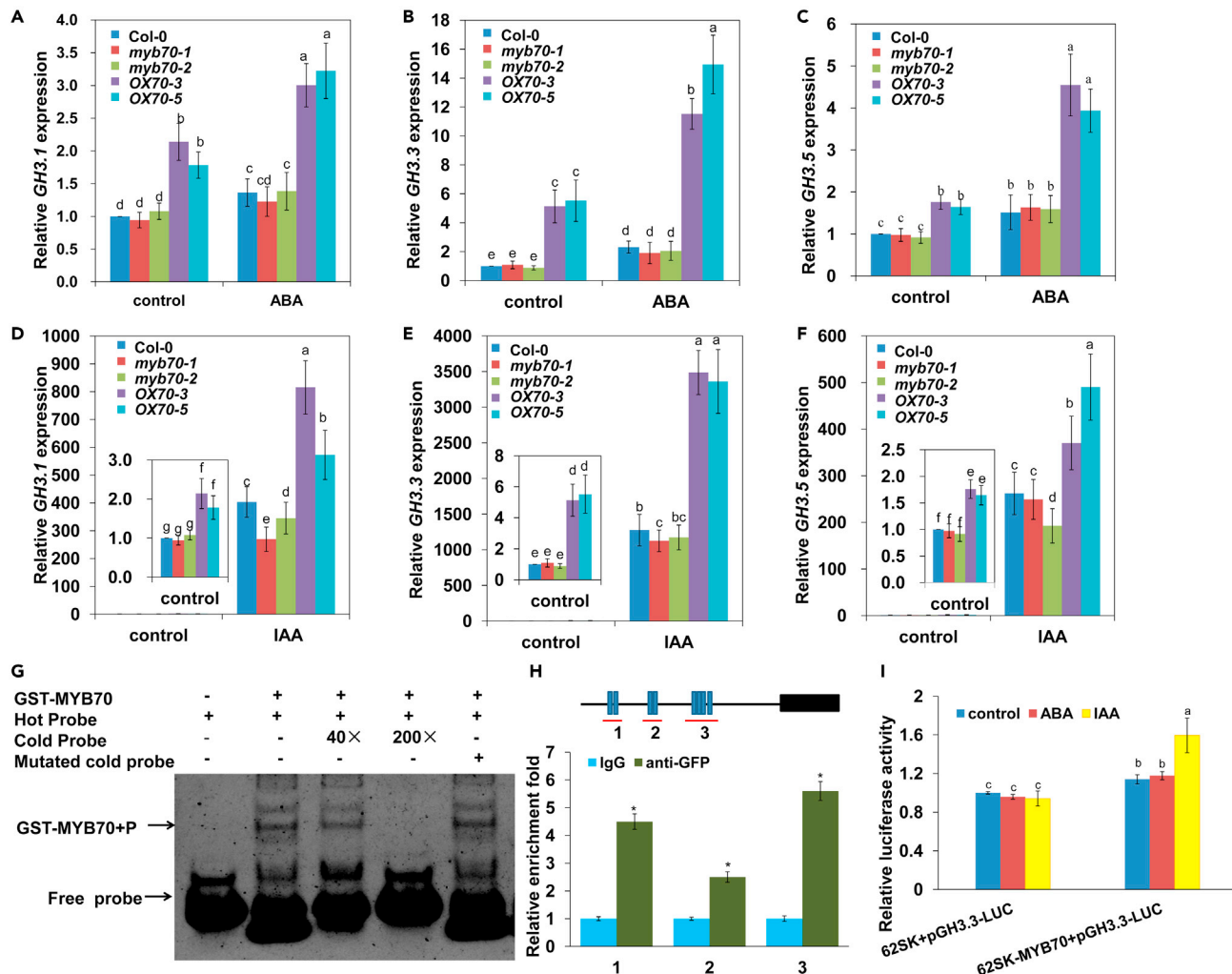
Figure 6. MYB70 positively regulates the expression of *GH3.1*, *GH3.3* and *GH3.5*

(A–F) Relative expression of the *GH3* genes in the roots of five-day-old Col-0, *myb70* mutant and *MYB70*-overexpressing *OX70* seedlings germinated on 1/2-strength MS medium and then transplanted to fresh medium supplemented with or without 10 μM abscisic acid (ABA) (A, B, C) or 10 μM indole-3-acetic acid (IAA) (D, E, F) for 24 h. Results shown are means ± SD (*n* = 3, more than 50 seedlings/genotype/repeat).

(G) EMSA detects the specific MYB70 binding to the *GH3.3* promoter region harboring MYB70-binding sites.

(H) ChIP-qPCR assay of the MYB70-DNA complexes. The schematic of the primer design for the ChIP-qPCR of the *GH3.3* promoter is shown at the top of the panel. The blue boxes on the black line represent the potential MYB70-binding sites, and the red lines mark sequences amplified by ChIP-qPCR. The promoter fragment enrichment assay following ChIP-qPCR was performed in the absence (IgG) or presence (anti-GFP) of anti-GFP antibody. Results shown are means ± SD (*n* = 3), and asterisks show significant differences from the control (IgG) (Student's *t*-test, *p* < 0.05).

(I) Transient dual-luciferase reporter assays indicate that MYB70 transcriptionally activated *GH3.3* expression without or with 5 μM ABA or 0.5 μM IAA. Results shown are means ± SD (*n* = 9). Different letters show significantly different values at *p* < 0.05 according to a Tukey's test. 62SK represents empty pGreenII 62-SK vector. 62SK-MYB70 represents the pGreenII 62-SK-MYB70 vector. pGH3.3-LUC represents pGreenII 0800-pGH3.3-LUC vector.

MYB70 modulates the ROS status in the roots by repressing the expression of *PER* genes independently of the UPB1 pathway

ROS play important roles in modulating root system development. The balance between $O_2^{\bullet-}$ and H_2O_2 in root tips controls PR growth and differentiation independently of the auxin signaling pathway (Tsukagoshi et al., 2010). Our transcriptome, qRT-PCR and GO enrichment analyses revealed that MYB70 down-regulated the expression of a set of *PER* genes and modulated the ROS metabolic process in the *OX70* plants (Figures S4A, S5 and S6). Several studies have demonstrated that overexpression of *PER34* or *PER57* resulted in longer PRs in overexpressor than in wild-type plants, whereas *per33 per34* double mutant lines presented shorter PRs than wild-type control (Passardi et al., 2005; Tsukagoshi et al., 2010). We next
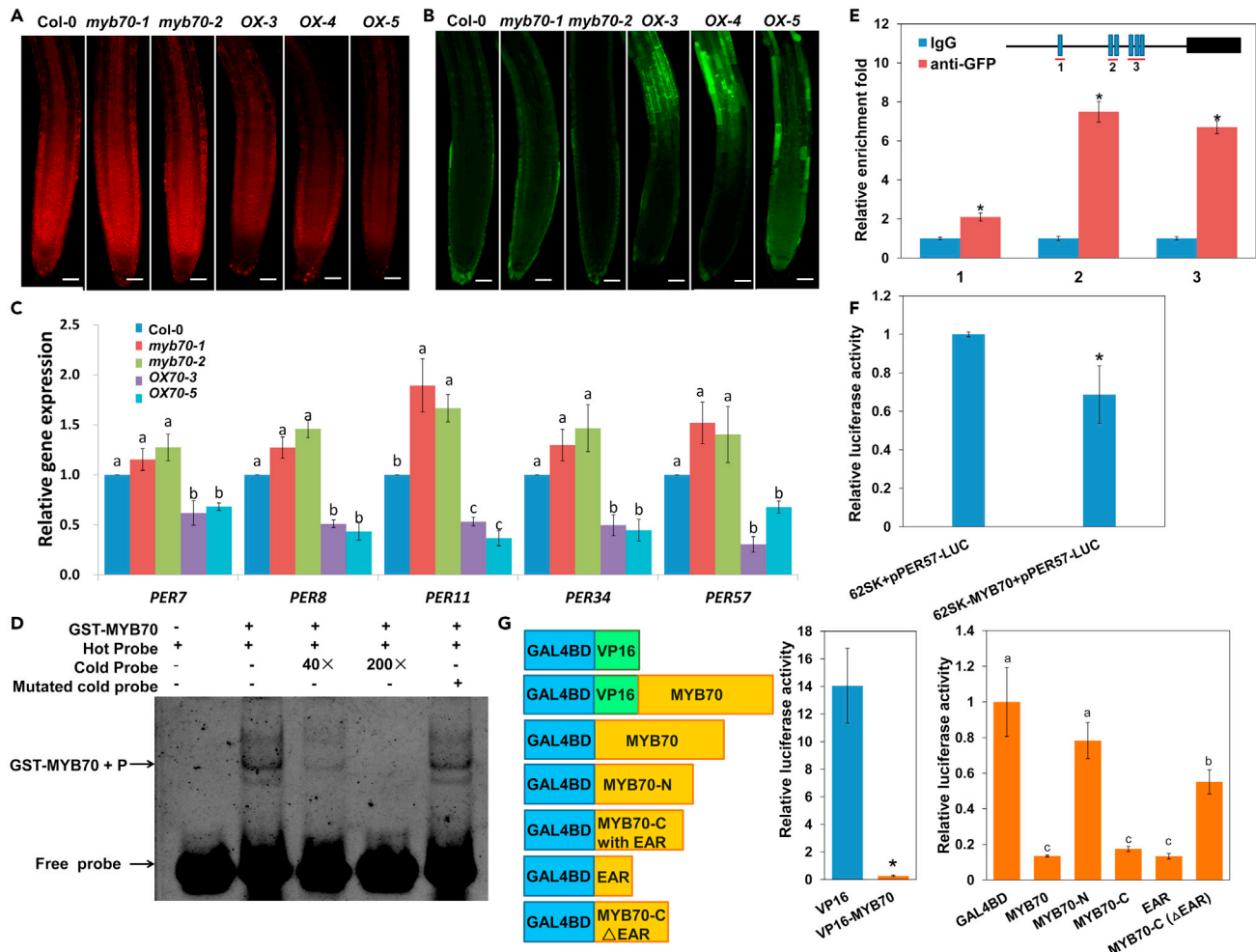
Figure 7. Overexpression of *MYB70* modulates $O_2^{\cdot-}$ and H_2O_2 balance in root tips by repressing the expression of *PER* genes

(A and B) Detection of endogenous $O_2^{\cdot-}$ production (A) and H_2O_2 (B) production in the root tips of five-day-old Col-0, *myb70* mutant and *OX70* seedlings (bar, 50 μm).

(C) Relative gene expression of the *PER7*, *PER8*, *PER11*, *PER34* and *PER57* genes in the roots of five-day-old Col-0, *myb70* and *OX70* seedlings. Results shown are means ± SD (*n* = 3, more than 50 seedlings/genotype/repeat).

(D) Specific binding of MYB70 to the *PER57* promoter region harboring MYB70-binding sites.

(E) ChIP-qPCR assay of the MYB70-DNA complexes. The blue boxes on the black line represent the potential MYB70-binding sites in the *PER57* promoter, and the red lines mark the sequences amplified by ChIP-qPCR. The promoter fragment enrichment assay following ChIP-qPCR was performed in the absence (IgG) or presence (anti-GFP) of anti-GFP antibody. Results shown are means ± SD (*n* = 3), and asterisks show significant differences from the control (IgG) (Student's *t*-test, *p* < 0.05).

(F) Transient dual-luciferase reporter assay shows repression of *PER57* expression by MYB70. Results shown are means ± SD (*n* = 9). 62SK, 62SK-MYB70 and pGreenII 62-SK-MYB70 represent empty pGreenII 62-SK, pGreenII 62-SK-MYB70 and pGreenII 0800-pPER57-LUC, respectively.

(G) Detection of the transcriptional repression activity of MYB70. Transcriptional activity assays in tobacco leaves (expressed in luciferase luminescence intensities) cotransfected with a pGreenII 0800-pUAS-35Smin-LUC reporter construct and one of the effector constructs fused with GAL4BD (schematic representation). The transcriptional activator VP16 was used as a positive control. MYB70-N (1–627); MYB70-C (628 to end, containing EAR motif); EAR (EAR motif-containing region 628 to 673); MYB70-C (ΔEAR) (MYB70-C without EAR motif, 673 to end). Results shown are means ± SD (*n* = 9). Asterisks show significant differences from the control (Student's *t*-test, *p* < 0.05). Different letters show significantly different values at *p* < 0.05 according to a Tukey's test.

measured ROS levels in *OX70*, *myb70*, and Col-0 root tips. Overexpression of *MYB70* reduced $O_2^{\cdot-}$ accumulation, especially in the root MZ, as indicated by the $O_2^{\cdot-}$-specific fluorescence probe dihydroethidium (DHE) (Figure 7A), whereas it increased H_2O_2 accumulation, especially in the EZ, as indicated by the H_2O_2-specific fluorescence probe BES-H_2O_2-AC (Figure 7B). Similarly, the diaminobenzene (DAB) staining (Figure S9) also showed that *OX70* plants accumulated higher levels of H_2O_2 in the root tips as compared with *myb70* mutants and Col-0 plants.

We then evaluated the expression of five *PER* genes in both roots and whole seedlings. As shown in Figures 7C and S6B, compared with the Col-0 plants, the *OX70* plants presented lower expression of these genes. Because overexpression of *PER57* resulted in PR elongation (Passardi et al., 2005; Tsukagoshi et al., 2010), we selected *PER57* as a representative gene to further test the direct relationship between MYB70 action and *PER* gene expression. First, we showed that MYB70 could directly bind to the promoter of *PER57* in a Y1H assay (Figure S10). Second, EMSA showed that MYB70 interacted with a 28-bp fragment that contained two MYB core sequences (CAACTAAT and TTGTTA) in the approximately −667- to −639-bp upstream of the starting codon in the *PER57* promoter region (Figure 7D). Third, ChIP-qPCR assay against *PER57* involving *35S:MYB70-GFP* transgenic plants confirmed the significant enrichment of MYB70-GFP-bound DNA fragments in the three regions of the promoter of *PER57* that contain 1–3 MYB core sequences (Figure 7E).

The above results indicated that MYB70 can directly bind to the *PER57* promoter, and the transcriptome and qRT-PCR results showed that *OX70* plants presented lower expression of *PER57* than the Col-0 plants did (Figures 7C–7E, S5, and S6). This finding is interesting as it suggests that MYB70 might also possess the transcriptional repression activity that could be attributed to the presence of a putative transcriptional repression motif, namely the ethylene-responsive element binding factor-associated amphiphilic repression (EAR) motif 'LXLSL' (Kagale et al., 2010; Persak and Pitzschke, 2014). To verify this hypothesis, we co-transfected the 35S:MYB70 plasmid and the PER57-LUC (pGreen II 0800-promoterPER57-Luciferase) reporter construct together in an LUC assay. Results of cotransfection shown in Figure 7F suggested that MYB70 indeed was able to repress the expression of *PER57* gene. These results collectively indicated that MYB70-mediated downregulation of the expression of *PER* genes resulted in increased $H_2O_2/O_2^{\bullet-}$ ratio, and suggested that MYB70 is a key player in modulating ROS status in plants.

Next, a dual-luciferase reporter system with positive control VP16 was used to further confirm the transcriptional repression activity of MYB70 (Figure 7G). The VP16 exhibited high luciferase (LUC) activity, whereas VP16-MYB70 fusion protein presented much lower activity than VP16 (Figure 7G, *Left*). Moreover, both the full-length MYB70 and the truncated MYB70-C (628 to end, containing EAR motif) constructs displayed significantly lower LUC activities than the negative control (GAL4BD), while the EAR motif-containing region (628–673) also showed similar inhibitory effect to that of the full-length MYB70 and the truncated MYB70-C constructs (Figure 7G, *Right*). In contrast, MYB70-N (1–627) showed no significant difference in LUC activity when compared with GAL4BD control (Figure 7G). We found that the truncated MYB70-C without the EAR motif (673 to end) also showed significant inhibitory effect on the pGAL4-LUC expression, implying that other inhibitory region(s) existed in this region. Collectively, these results demonstrated that MYB70 acted as a transcriptional repressor and the EAR motif was required for the transcriptional repression activity.

The bHLH TF-encoding *UPB1* plays a critical role in modulating the balance between differentiation and proliferation in the roots by regulating ROS equilibrium (Tsukagoshi et al., 2010). The above results (Figures 7A, 7B and S9) showed that the phenotype resulted from *MYB70* overexpression was similar to that of *UPB1*-overexpressing plants (Tsukagoshi et al., 2010). Our RNA-seq, qRT-PCR, and Y2H analyses revealed that MYB70-mediated *PER* gene expression occurred independently of UPB1 (Figure S11; Data S1 and S2). Together, these results suggested that MYB70-mediated root growth via repression of *PER* genes is independent of the UPB1 pathway.

MYB70 negatively regulates suberin biosynthesis in roots

Another finding from the transcriptome analysis of particular interest was that the expression of several genes involved in suberin biosynthesis, such as *GPAT5*, *GPAT7*, *CYP86A1*, *CYP86B1*, *CYP86B2*, and *FACT*, and the expression of the cuticular wax biosynthesis-related gene *WSD7* were downregulated in the *OX70* plants (Figure S5), as also evidenced by the results of qRT-PCR analysis (Figures 8A and S6C). In comparison with the Col-0 plants, the *OX70* plants presented lower expression levels of these six genes (Figures 8A and S6C), suggesting a negative feedback regulation of suberin and/or cuticular wax biosyntheses by MYB70.

To investigate whether MYB70 could directly regulate the expression of suberin biosynthesis-related gene(s), we performed the following assays with a representative gene, the *GPAT5*, whose loss-of-function presented decreased suberin deposition in their young roots and seed coats (Beisson et al., 2007). First, we
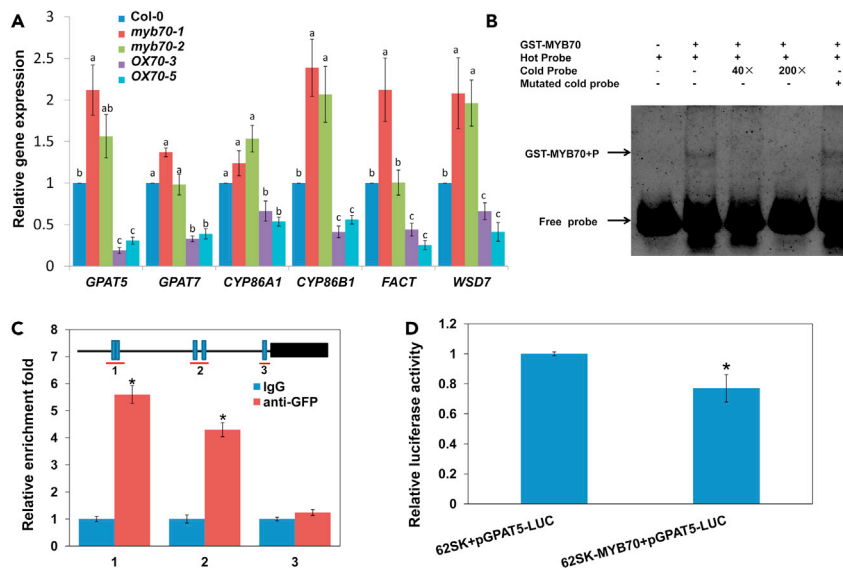
Figure 8. Overexpression of *MYB70* repressed the expression of genes encoding the enzymes involved in wax, cutin and suberin biosynthesis

(A) Relative expression of the *GPAT5*, *GPAT7*, *CYP86A1*, *CYP86B1*, *FACT* and *WSD7* genes in the roots of five-day-old *Arabidopsis* Col-0, *myb70* mutant and *MYB70*-overexpressing *OX70* seedlings. Results shown are means ± SD (n = 3, more than 50 seedlings/genotype/repeat).

(B) EMSA detects the specific binding of MYB70 to the *GPAT5* promoter region harboring MYB70-binding sites.

(C) ChIP-qPCR assay of the MYB70-DNA complexes. The schematic of the primer design for the *GPAT5* promoter is shown at the top of the panel. The blue boxes on the black line represent the potential MYB70-binding sites, and the red lines mark sequences amplified by ChIP-qPCR. The promoter fragment enrichment assay following ChIP-qPCR was performed in the absence (IgG) or presence (anti-GFP) of anti-GFP antibody. Results shown are means ± SD, and asterisks show significant differences from the control (IgG) (Student's *t*-test, $p < 0.05$).

(D) Transient dual-luciferase reporter assays indicate that MYB70 repressed *GPAT5* expression. 62SK represents empty pGreenII 62-SK vector. 62SK-MYB70 represents the pGreenII 62-SK-MYB70 vector. pGPAT5-LUC represents pGreenII 0800-pGPAT5-LUC vector. *Renilla* luciferase (REN) was used for normalization. Results shown are means ± SD (n = 9). Asterisks show significant differences from the control (Student's *t*-test, $p < 0.05$). Different letters show significantly different values at $p < 0.05$ according to a Tukey's test.

found that MYB70 bound to its promoter using a Y1H assay (Figure S12). Second, EMSA subsequently revealed that MYB70 interacted with a 32-bp fragment that contained two adjacent MYB core sequences (TAGTTTTGTTA) in the approximately −1,320- to −1309-bp upstream of the starting codon in the promoter region of the *GPAT5* (Figure 8B). Third, the physical interaction was also confirmed by the ChIP-qPCR assay against *GPAT5* using the *35S:MYB70-GFP* transgenic plants. As shown in Figure 8C, significant enrichment of MYB70-GFP-bound DNA fragments was detected in the two regions of the *GPAT* promoter, each of which contains 2 MYB core sequences. Finally, we examined the transcriptional repression activity of MYB70 using the dual-luciferase reporter system. As shown in Figure 8D, cotransfection of 35S:MYB70 with the reporter construct repressed LUC activity of pGreen II 0800-promoterGPAT5-LUC.

Since *gpat5* loss-of-function mutants presented decreased suberin deposition in their young roots and seed coats (Beisson et al., 2007), *cyp86A1* mutants showed reduced suberin composition in their roots (Höfer et al., 2008), and *cyp86B1* mutants displayed a novel change in composition of suberin monomers (Compagnon et al., 2009). We, thus, suspected that compared with Col-0, *OX70* might have a lower suberin deposition which could affect the growth and development of *OX70*, because suberin is a lipid-phenolic biopolyester that is present in cell walls and modulates root growth, water and ion uptake by the roots (Compagnon et al., 2009; Tylová et al., 2017). To test this hypothesis, we first investigated suberin deposition in the roots of the *OX70*, *myb70*, and Col-0 plants. Using the suberin histochemical lipophilic dye Sudan black B (Beisson et al., 2007), we found that compared with the *myb70* and Col-0 roots, the *OX70* roots presented less staining intensity (Figure 9A). The root suberization was then confirmed using fluorol yellow (FY) staining (Naseer et al., 2012). A striking reduction in suberization was observed in the *OX70*
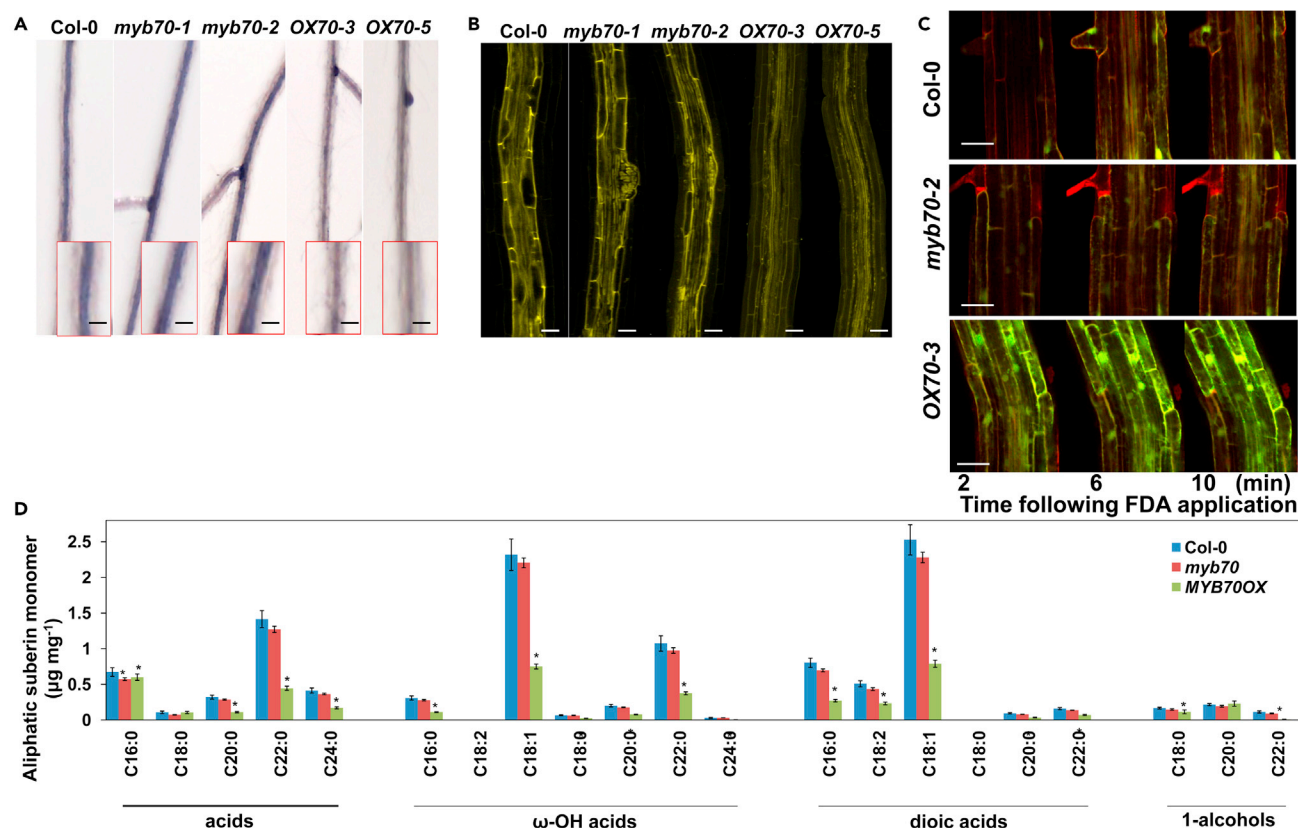
Figure 9. Overexpression of *MYB70* reduced suberin deposition in the roots

(A and B) Detection of suberin deposition in the roots using the suberin histochemical lipophilic dye Sudan black B (bar, 50 μm) (A) and fluorol yellow staining (bar, 50 μm) (B) of the roots of nine-day-old *Arabidopsis* Col-0, *myb70* mutant and *MYB70*-overexpressing *OX70* seedlings germinated on 1/2-strength MS medium.

(C) Fluorescein diacetate penetration across cell layers of the roots of Col-0, *myb70* and *OX70* seedlings (bar, 50 μm).

(D) Detection of root suberin chemical composition in the roots of five-day-old Col-0, *myb70* mutant and *OX70* seedlings germinated on 1/2-strength MS medium using gas chromatography flame ionization detection. Results shown are means ± SD ($n = 4$, more than 250 plants/genotype/repeat). Different letters show significantly different values at $p < 0.05$ according to a Tukey's test.

roots (Figure 9B). To confirm these results, we then investigated whether a disruption of root suberization affected the uptake and transport of the fluorescent tracer fluorescein diacetate (FDA). After application of FDA, fluorescence was detected only slightly in the roots of the Col-0 and *myb70* seedlings, whereas FDA accumulation was much higher in the roots of the *OX70* seedlings (Figure 9C). These results suggested that MYB70 increased the uptake ability by repressing root suberization. To address this phenomenon, we next investigated the macronutrient and micronutrient contents in the roots and shoots of *OX70*, *myb70* and Col-0. The *myb70* mutant did not exhibit any significant changes in the contents of the measured elements in either roots or leaves (Figure S13). However, in the *OX70* plants, the contents of manganese (Mn), iron (Fe) and copper (Cu) significantly increased in the roots (Figure S13A), and the contents of potassium (K) and Mn significantly increased in the leaves (Figure S13B), while the leaf Cu level significantly decreased (Figure S13B).

To further confirm that *MYB70* affected root suberization, we detected suberin chemical composition in roots of *OX70*, *myb70*, and Col-0 plants using gas chromatography flame ionization detection (GC-FID). There were no significant differences in the contents of the total aliphatic suberin monomer between *myb70* and Col-0 roots; however, the total aliphatic suberin monomer was 60.7% lower in *OX70* roots than in Col-0 roots. This difference was due to a general decrease in almost all major suberin monomer constituents, including the significant decreases in C16:0, C20:0, C22:0, and C24:0 acids, C16:0, C18:1, C18:0, C20:0, C22:0, and C24:0 ω-OH acids, C16:0, C18:2, C18:1, C20:0, and C22:0 dioic acids, and C18:0 and

C22:0 1-alcohols (Figure 9D). These results together indicated that the overexpression of *MYB70* reduced suberin deposition in roots of the *OX70* plants.

DISCUSSION

Elucidation of the crosstalk and balance among signaling molecules, like ABA, auxin, and ROS as well as their interactions in modulating plant growth and stress tolerance, has always been an important topic in botanical studies (Zhou et al., 2018). Here, analysis of the phenotypes of *OX70* and *myb70* plants at different developmental stages revealed various roles of MYB70 in responses to phytohormone signaling and developmental processes. In germinating seeds of various combinations of *MYB70* and *ABI5* overexpressor or mutant plants, the interaction of ABA-induced MYB70 and ABI5 improved ABI5's ability to transcriptionally regulate its target genes by increasing ABI5 protein stabilization, thereby modulating seed germination in response to ABA. Furthermore, the underlying mechanisms involved direct regulation of the expression of *GH3.3*, *PER57*, and *GPAT5* by MYB70's dual transcriptional regulatory activities, which in turn modulate auxin signaling, ROS balance, and suberization in the roots, thereby affecting growth and development of the root system.

MYB70 negatively regulates seed germination in response to ABA by interacting with ABI5

Phenotypic analyses revealed that MYB70 negatively regulated seed germination in response to ABA (Figure 1). Moreover, ABA levels in *OX70* and *myb70* plants were unaltered (Figure 3C), suggesting that MYB70 modulates seed germination by regulating ABA signaling but not by affecting ABA biosynthesis. We thus searched for MYB70-interacting proteins or transcriptional regulators, particularly those participated in ABA-mediated regulation of seed germination, and identified ABI5. ABI5 acts as a central TF that is involved in ABA-mediated seed germination (Zhao et al., 2018; Zhou et al., 2015). Many studies have revealed ABI5-mediated signaling and regulatory mechanisms of ABI5-interacting proteins (Ju et al., 2019; Reeves et al., 2011). In recent years, with the continual discovery of ABI5-interacting proteins and the elucidation of their functions (Chang et al., 2019; Reeves et al., 2011; Zhao et al., 2018; Zhou et al., 2015), understanding of the molecular basis underlying the ABI5-mediated ABA transcriptional regulatory network has continually improved. In the present study, using Y2H, *in vitro* pull-down, Co-IP and BiFC assays, we identified the ABA-inducible R2R3 MYB TF MYB70 as a new ABI5-interacting protein (Figure 2). Subsequently, genetic analysis revealed that MYB70 additively regulated seed germination in response to ABA together with ABI5 (Figures 1 and 3). Results of the qRT-PCR and cotransfection assays indicated that MYB70 interacts with ABI5, resulting in improved ABI5's ability to upregulate the expression of its target genes, *EM1* and *EM6* (Figures 3A, 3B, 3D and 3E). Furthermore, immunoblotting analysis showed that MYB70 increases ABI5 stabilization after the removal of ABA from germinating *Arabidopsis* seeds. Taken together, these data indicated that the interaction between MYB70 and ABI5 increases ABI5 protein stabilization; and thus helps in modulating ABI5-regulated seed germination in response to ABA signaling.

ABA-inducible MYB70 integrates auxin signaling to modulate root system development

The expression patterns of the members of R2R3 MYB subgroup S22, including MYB44, MYB70, MYB73, and MYB77, in response to ABA are similar in the roots (Figures 1C and 1D) (Persak and Pitzschke, 2014). Similar to those occurred in *MYB44*-overexpressing (*OX44*) (Jung et al., 2008) and *MYB77*-overexpressing (*OX77*) *Arabidopsis* plants (Shin et al., 2007), the PRs were shorter in *OX70* plants than in Col-0 plants, while the knockout mutants (*myb70*, *myb44* and *myb77*) exhibited no obvious phenotypic differences (Figures 4A and 4B) (Jung et al., 2008; Shin et al., 2007). Furthermore, in most of the assays, we observed that the phenotypic effects on the roots of *myb70* plants were weak (Figure 4), suggesting that functional redundancy of R2R3 MYB subgroup S22 TFs occurs in the modulation of root growth and development (Lashbrooke et al., 2016).

Interestingly, we found that in contrast to *OX77* plants that showed an increased auxin response, as indicated by the GUS staining of *OX77/DR5:GUS* plants (Shin et al., 2007), both the GUS staining of *OX70/DR5:GUS* plants and the GFP fluorescence of *OX70/DR5:GFP* plants showed decreased intensities of these two markers (Figures 5E and 5F). We thus examined free IAA levels and found that overexpression of *MYB70* did not affect the free IAA levels in the *OX70* plants (Figure 5G). However, our detailed examination indicated that overexpression of *MYB70* increased the conjugated IAA levels in the *OX70* plants (Figure 5G), suggesting that *MYB70* may play a role in maintaining auxin homeostasis, and thus auxin signaling in plants. Subsequent transcriptome and qRT-PCR analyses revealed that MYB70 upregulated the expression

of several ABA-inducible *GH3* genes, including *GH3.1*, *GH3.3*, and *GH3.5* (Figures 6A–6F). Further analyses using Y1H, EMSA, and ChIP-qPCR assays indicated that MYB70 upregulated *GH3.3* transcription by directly binding to its promoter (Figures 6G, 6H and S7), which was supported by a transcriptional activity assay using dual-luciferase reporter system (Figure 6I). The ABA-inducible *GH3* genes encode IAA-conjugating enzymes whose activities result in IAA inactivation (Park et al., 2007). Growth of the root systems of *GH3*-overexpressing plants, such as *GH3.5 OX* plants, was shown to be reduced (Park et al., 2007; Seo et al., 2009), which is similar to the phenotype of *OX70* plants (Figure 4). In support of our results, overexpression of the ABA-inducible *MYB96* modulated RSA by upregulating the expression of *GH3.3* and *GH3.5* genes, and as a consequence increasing the conjugated IAA levels; however, it did not alter the free IAA levels in transgenic *Arabidopsis OX96* plants (Seo et al., 2009). The stable levels of free IAA in *OX70*, *OX77*, and *OX96* plants suggested a rigorous control of auxin homeostasis in plants to regulate root growth (Park et al., 2007; Seo et al., 2009).

In addition to PR growth, overexpression of *MYB70* also markedly reduced LR formation, especially LR elongation, as indicated by the reduced number of LRPs in stages III and IV (Figure 4J). These results support the hypothesis that *MYB70* integrates ABA and auxin signaling to modulate root system growth and development through a negative feedback regulation of auxin homeostasis by upregulating ABA-inducible *GH3* gene expression, and also indicate that there exist functional differences between MYB70 and MYB77 in modulating the auxin signaling pathway.

Involvement of MYB70 in modulating the $H_2O_2/O_2^{\cdot-}$ ratio in the root tips and subsequent root system development

Modulation of PER activities and ROS levels affects stem cell fate and the balance between differentiation and proliferation in plants (Tsukagoshi et al., 2010). Our transcriptome and qRT-PCR analyses indicated that MYB70 represses the expression of a set of *PER* genes (Figures 7C and S6B). Furthermore, Y1H, EMSA, and ChIP-qPCR analyses subsequently revealed that MYB70 could directly bind to the *PER57* promoter, as a representative example, suggesting that *PER* genes are downstream target of MYB70 (Figures 7D, 7E and S10). Moreover, the transcriptional activity analysis revealed that MYB70 acts as a transcriptional repressor (Figure 7G), downregulating the expression of *PER57* (Figure 7F). This result along with that described above for the transcriptional activity assay of the *GH3.3* gene indicate that MYB70 has dual transcriptional activities, and can act as both activator and repressor to regulate the expression of its downstream genes. However, when the activation function and when the repression function act, this required further investigations. The dual functions of TFs in activation or repression of different target genes through direct physical interaction is an interesting phenomenon that has been reported previously, such as for ABI4. ABI4 modulates seed dormancy by directly repressing the transcription of *ARR6*, *ARR7*, and *ARR15* (Huang et al., 2017), and reducing ABA degradation through direct repression of the expression of *CYP707A1* and *CYP707A2*, while promoting GA degradation through direct activation of *GA2ox7* expression (Shu et al., 2016a, 2016b). In addition, ABI4 also modulates flowering by directly activating *Flowering Locus C* (*FLC*) expression (Shu et al., 2016b), while it modulates ROS levels by directly repressing *Vitamin C Defective 2* (*VTC2*) expression in *Arabidopsis* (Yu et al., 2019). Results of this study, at least, suggest that both the activation and repression functions of MYB70 were activated in parallel for regulation of PR growth of *Arabidopsis* seedlings through the auxin and ROS signaling pathways (Figures 6 and 7). In addition, considering that MYB70 is a transcriptional repressor with a repression activity of EAR motif (Figure 7G), a co-activator might be required along with MYB70 to activate the expression of *GH3* genes. This co-activator should also be able to overcome the repression activity of MYB70. It will then be interesting to discover detailed molecular mechanisms for the dual activities of MYB70 in regulation of plant growth and development in a spatiotemporal manner.

PERs regulate ROS status in two opposite ways, namely reduction of H_2O_2 by transferring electrons to donor molecules and formation of $O_2^{\cdot-}$ by catalyzing the hydroxylic cycle (Passardi et al., 2005; Pitzschke et al., 2006; Tsukagoshi et al., 2010). In *OX70* plants, repression of *PER* gene expression led to decreased $O_2^{\cdot-}$ and increased H_2O_2 accumulation in the roots, especially in the EZ (Figures 7A, 7B and S9). Although the phenotype of the PRs of *OX70* was similar to that of 35S:*UPB1* (*UPB1OX*), our results revealed that the repression of *PER* gene expression by MYB70 occurred independently of UPB1 (Figure S11). These findings showed that various pathways are involved in the regulation of $H_2O_2/O_2^{\cdot-}$ ratio to maintain apical meristem activity in the root tips, and MYB70 pathway regulates ROS status at least independently of the UPB1 pathway.

In addition to modulating cell proliferation and differentiation, PER-mediated ROS status also plays a role in the modification of cell wall structure and initiation of cell expansion, thereby regulating root growth (Passardi et al., 2005; Tsukagoshi et al., 2010). Our transcriptome analysis revealed that in addition to *PER* genes, MYB70 also repressed the transcription of many other genes participated in modifying cell wall structure, such as *Laccases* (*LACs*), *Xyloglucan Endotransglucosylase/Hydrolases* (*XTHs*) and *Extensins* (*EXTs*) (Figure S5). Both PERs and LACs play roles in monolignol unit oxidation, which is responsible for the final step of lignin assembly, thereby modulating cell size and number (Passardi et al., 2004). In support of these data, *OX70* plants showed reduced MZ cell number, the length of MZ and EZ, and the cell length in transition zones (Figures 4C–4G). Taken together, these results indicated that MYB70, at least in part, downregulated the expression of *PER* genes and cell wall structure-related genes, thereby altering root system growth.

MYB70 and root suberization

As a component of the plant secondary cell wall, suberin is deposited between the plasma membrane and primary cell wall to form lamellae (Barberon et al., 2016; Compagnon et al., 2009; Yadav et al., 2014). In the roots, suberin is deposited on the endodermal surface and Casparian strip to form an extracellular diffusion barrier to modulate water and ion transport (Andersen et al., 2015; Barberon et al., 2016). Therefore, modulation of suberin deposition in the roots alters root cell structure and physiology (Enstone and Peterson, 2005). Roots have evolved the capability to modulate their suberization to adapt to environmental cues (Yadav et al., 2014). Our results provided evidence that the reduced endodermal suberization in *OX70* roots increased root uptake and transport abilities (Figures 9 and S13). Detection of nutrient contents revealed an increased abundance of Mn, Fe, and Cu in the roots (Figure S13A) and an increased abundance of K and Mn in the leaves of *OX70* plants (Figure S13B), suggesting that the decreased suberin deposition in *OX70* roots improved the uptake of these macronutrients and micronutrients by the roots. The result of ionomic profiling was also supported by the sharp increase in FDA fluorescent tracer in *OX70* roots (Figure 9C). However, although overexpression of *MYB70* increased the Cu content in the roots (Figure S13A), it decreased the Cu content in the leaves (Figure S13B), indicating reduced Cu transport from the roots to the leaves by the function of MYB70. These findings were also consistent with those published by previous reports that showed that disrupted endodermal suberization differentially affected element uptake and transport ability which, therefore, should be interesting for further elucidation (Barberon et al., 2016; Cohen et al., 2020).

Previous studies have demonstrated a correlation between ABA and suberization in plants (Barberon et al., 2016; Yadav et al., 2014). We showed here that ABA-induced MYB70 reduced suberin deposition in the roots by repressing the expression of genes involved in suberin biosynthesis (Figures 8 and 9). Further studies using Y1H, EMSA, and ChIP-qPCR analyses confirmed that MYB70 directly bound to the promoter of the suberin biosynthesis-related *GPAT5* gene (Figures 8B, 8C and S12). In addition, the transcriptional activity assay using dual-luciferase reporter system revealed that MYB70 downregulated *GPAT5* via its transcriptional repression activity (Figure 8D). Taken together, these results indicated that MYB70 acts as a negative regulator of suberization in an ABA-dependent manner.

Suberin biosynthesis follows a PER-mediated oxidative coupling process (Bernards et al., 2004; Passardi et al., 2004). Therefore, the altered expression of the *PER* genes by MYB70 also influences the modulation of suberin biosynthesis. Overall, MYB70 reduced suberization by downregulating the expression of genes encoding PERs and suberin biosynthesis-related genes, thereby altering root growth.

In summary, our findings revealed various functions of MYB70 in the modulation of plant growth and development. In seeds, MYB70 was shown to interact with ABI5 both *in vitro* and *in vivo*, and the interaction increased ABI5 stabilization; and thus, improved ABI5's ability to transcriptionally modulate its target genes. In the roots, ABA-induced MYB70 modulated auxin signaling by increasing the content of conjugated IAA. In addition, MYB70 negatively regulated the expression of *PER* genes and suberin biosynthesis-related genes, thereby modulating ROS balance and decreasing suberization in the roots, which ultimately affected RSA (Figure 10). Our results might also open an avenue for creating new crop varieties with improved water and nutrient use efficiency through genetic engineering of *MYB* genes, which are suitable for sustainable agriculture in an era of climate change.

Limitations of the study

In seed germination assay, *myb70* seeds displayed decreased sensitivity, while *OX70* seeds showed increased sensitivity in response to exogenous ABA. However, in root system growth, the phenotypic
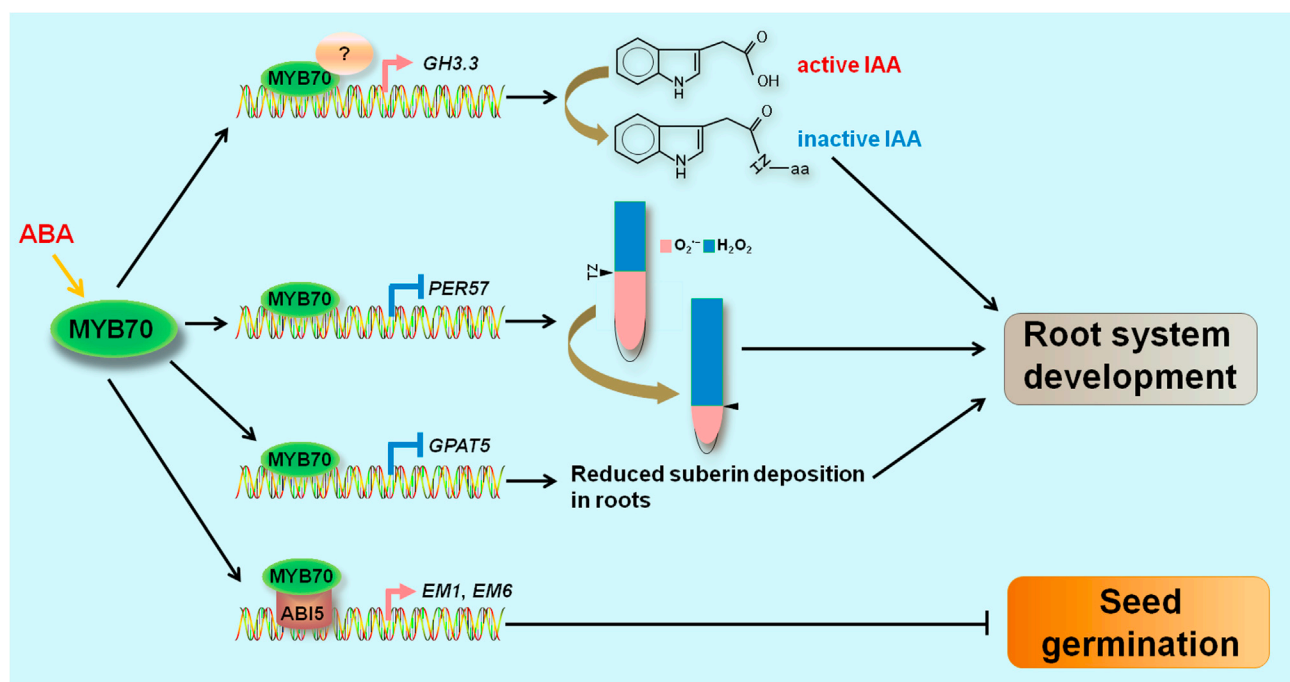
Figure 10. Proposed model of ABA-mediated seed germination and root system development via the MYB70 integrator

The interaction of ABA-induced MYB70 and ABI5 improves ABI5's ability to transcriptionally regulate its target genes by increasing ABI5 protein stabilization, thereby inhibiting seed germination in response to ABA. Moreover, ABA-induced MYB70 represses auxin signaling by increasing inactive IAA levels through the direct upregulation of *GH3.3* expression via interaction with an unknown transcriptional activator. MYB70 modulates $O_2^{\cdot-}$ and H_2O_2 balance in the root tips via its transcriptional repression of *PER57* gene expression. Increased *MYB70* expression reduces root suberization by directly downregulating *GPAT5* expression via its transcriptional repression activity, thereby ultimately inhibiting PR growth.

effects of *myb70* plants were weak, suggesting that there may be functional redundancy among the R2R3 MYB subgroup S22 TFs in the modulation of root growth. Further studies using multiple mutants will enable us to understand the role of MYB70 and other members of the R2R3 MYB subgroup S22 in regulation of root growth and suberization.

STAR★METHODS

Detailed methods are provided in the online version of this paper and include the following:

- KEY RESOURCES TABLE
- RESOURCE AVAILABILITY
  - Lead contact
  - Materials availability
  - Data and code availability
- EXPERIMENTAL MODEL AND SUBJECT DETAILS
  - Arabidopsis thaliana
  - Bacterial strains
- METHOD DETAILS
  - Phenotypic analysis
  - Plasmid construction and transformation
  - Seed germination analysis
  - qRT-PCR and transcriptome analyses
  - *In vitro* pull-down, Y1H, and Y2H assays
  - Co-IP analysis
  - ChIP assays
  - BiFC assay
  - Immunoblotting analysis

- ○ Dual-luciferase (LUC) reporter assays
- ○ Quantification of endogenous ABA and IAA level
- ○ Fluorescence microscopy
- ○ Penetration assay
- ○ Histological analysis
- ○ Root suberin chemical composition analysis
- ○ Metal element content analysis
- ○ Accession numbers
- ● QUANTIFICATION AND STATISTICAL ANALYSIS

AUTHOR CONTRIBUTIONS

J.X. designed and supervised the research. J.W. performed most experiments. R.W. performed Y1H and Y2H experiments. P.Z. and L.S. characterized the phenotypes and constructed vectors. S.L. and H.D. performed chemical composition analysis. Q.J. performed planting. J.W., L.-S.T., and J.X. analyzed the data and wrote the manuscript.

DECLARATION OF INTERESTS

The authors declare no competing interests.

REFERENCES

Andersen, T., Barberon, M., and Geldner, N. (2015). Suberization-the second life of an endodermal cell. Curr.Opin. Plant Biol. *28*, 9–15.

Barberon, M., Vermeer, J., De Bellis, D., Wang, P., Naseer, S., Andersen, T., Humbel, B., Nawrath, C., Takano, J., Salt, D.E., et al. (2016). Adaptation of root function by nutrient-induced plasticity of endodermal differentiation. Cell *164*, 447–459.

Beisson, F., Li-Beisson, Y., Bonaventure, G., Pollard, M., and Ohlrogge, J. (2007). The acyltransferase GPAT5 is required for the synthesis of suberin in seed coat and root of *Arabidopsis*. Plant Cell *19*, 351–368.

Berhin, A., Bellis, D., Franke, R., Buono, R., Nowack, M., and Nawrath, C. (2019). The root cap cuticle: a cell wall structure for seedling establishment and lateral root formation. Cell *176*, 1–12.

Bernards, M., Summerhurst, D., and Razem, F. (2004). Oxidases, peroxidases and hydrogen peroxide: the suberin connection. Phytochem. Rev. *3*, 113–126.

Bu, Q., Li, H., Zhao, Q., Jiang, H., Zhai, Q., Zhang, J., Wu, X., Sun, J., Xie, Q., Wang, D., et al. (2009). The *Arabidopsis* RING finger E3 ligase RHA2a is a novel positive regulator of abscisic acid signaling during seed germination and early seedling development. Plant Physiol. *150*, 463–481.

Casamitjana-Martınez, E., Hofhuis, H.F., Xu, J., Liu, C.-M., Heidstra, R., and Scheres, B. (2003). Root-specific *CLE19* overexpression and the *sol1/2* suppressors implicate a CLV-like pathway in the control of *Arabidopsis* root meristem maintenance. Curr. Biol. *13*, 1435–1441.

Chang, G., Yang, W., Zhang, Q., Huang, J., Yang, Y., and Hu, X. (2019). ABI5-BINDING PROTEIN 2 coordinates CONSTANS to delay flowering by recruiting the transcriptional corepressor TPR2. Plant Physiol. *179*, 477–490.

Coen, O., Lu, J., Xu, W., Vos, D., Péchoux, C., Domergue, F., Grain, D., Lepiniec, L., and Magnani, E. (2019). Deposition of a cutin apoplastic barrier separating seed maternal and zygotic tissues. BMC Plant Biol. *19*, 304.

Cohen, H., Fedyuk, V., Wang, C., Wu, S., and Aharoni, A. (2020). SUBERMAN regulates developmental suberization of the *Arabidopsis* root endodermis. Plant J. *102*, 431–447.

Compagnon, V., Diehl, P., Benveniste, I., Meyer, D., Schaller, H., Schreiber, L., Franke, R., and Pinot, F. (2009). CYP86B1 is required for very long chain ω-hydroxyacid and α, ω-dicarboxylic acid synthesis in root and seed suberin polyester. Plant Physiol. *150*, 1831–1843.

Ding, S., Zhang, B., and Qin, F. (2015). Arabidopsis RZFP34/CHYR1, a ubiquitin E3 ligase, regulates stomatal movement and drought tolerance via SnRK2.6-mediated phosphorylation. Plant Cell *27*, 3228–3244.

Enstone, D., and Peterson, C. (2005). Suberin lamella development in maize seedling roots grown in aerated and stagnant conditions. Plant Cell Environ *28*, 444–455.

Fernández-Marcos, M., Desvoyes, B., Manzano, C., Liberman, L.M., Benfey, P.N., del Pozo, J.C., and Gutierrez, C. (2017). Control of Arabidopsis

lateral root primordium boundaries by MYB36. New Phytol. *213*, 105–112.

Finkelstein, R.R., and Lynch, T. (2000). The *Arabidopsis* abscisic acid response gene *ABI5* encodes a basic leucine zipper transcription factor. Plant Cell *12*, 599–609.

Friml, J., Vieten, A., Sauer, M., Weijers, D., Schwarz, H., Hamann, T., Offringa, R., and Jürgens, G. (2003). Efflux-dependent auxin gradients establish the apical-basal axis of *Arabidopsis*. Nature *426*, 147–153.

Guan, C., Wang, X., Feng, J., Hong, S., Liang, Y., Ren, B., and Zuo, J. (2014). Cytokinin antagonizes abscisic acid-mediated inhibition of cotyledon greening by promoting the degradation of ABSCISIC ACID INSENSITIVE5 protein in Arabidopsis. Plant Physiol. *164*, 1515–1526.

Gutierrez, L., Mongelard, G., Floková, K., Pacurar, D., Novak, O., Staswick, P., Kowalczyk, M., Pacurar, M., Demailly, H., Geiss, G., et al. (2012). Auxin controls *Arabidopsis* adventitious root initiation by regulating jasmonic acid homeostasis. Plant Cell *24*, 2515–2527.

Hagen, G., and Guilfoyle, T. (2002). Auxin-responsive gene expression: genes, promoters and regulatory factors. Plant Mol. Biol. *49*, 373–385.

Hellens, R., Allan, A., Friel, E., Bolitho, K., Grafton, K., Templeton, M., Karunairetnam, S., Gleave, A., and Laing, W. (2005). Transient expression vectors for functional genomics, quantification of promoter activity and RNA silencing in plants. Plant Methods *1*, 13.

Hirayama, T., and Shinozaki, K. (2007). Perception and transduction of abscisic acid signals: keys to the function of the versatile plant hormone ABA. Trends Plant Sci. *12*, 343–351.

Höfer, R., Briesen, I., Beck, M., Pinot, F., Schreiber, L., and Franke, R. (2008). The *Arabidopsis* cytochrome P450 *CYP86A1* encodes a fatty acid ω-hydroxylase involved in suberin monomer biosynthesis. J. Exp. Bot. *59*, 2347–2360.

Holbein, J., Shen, D., and Andersen, T. (2021). The endodermal passage cell – just another brick in the wall? New Phytol. *230*, 1321–1328.

Hossain, M.A., Bhattacharjee, S., Armin, S.M., Qian, P., Xin, W., Li, H.Y., Burritt, D.J., Fujita, M., and Tran, L.S. (2015). Hydrogen peroxide priming modulates abiotic oxidative stress tolerance: insights from ROS detoxification and scavenging. Front. Plant Sci. *6*, 420–435.

Huang, X., Zhang, X., Gong, Z., Yang, S., and Shi, Y. (2017). ABI4 represses the expression of type-A ARRs to inhibit seed germination in *Arabidopsis*. Plant J. *89*, 354–365.

Ju, L., Jing, Y., Shi, P., Liu, J., Chen, J., Yan, J., Chen, K., and Sun, J. (2019). JAZ proteins modulate seed germination through interacting with ABI5 in bread wheat and *Arabidopsis*. New Phytol. *223*, 246–260.

Jung, C., Seo, J.S., Han, S., Koo, Y., Kim, C., Song, S., Nahm, B., Choi, Y., and Cheong, J.J. (2008). Overexpression of *AtMYB44* enhances stomatal closure to confer abiotic stress tolerance in transgenic Arabidopsis. Plant Physiol. *146*, 623–635.

Kagale, S., Links, M.G., and Rozwadowski, K. (2010). Genome-wide analysis of ethylene-responsive element binding factor-associated amphiphilic repression motif-containing transcriptional regulators in *Arabidopsis*. Plant Physiol. *152*, 1109–1134.

Kelemen, Z., Sebastian, A., Xu, W., Grain, D., Salsac, F., Avon, A., Berger, N., Tran, J., Dubreucq, B., Lurin, C., et al. (2015). Analysis of the DNA-binding activities of the Arabidopsis R2R3-MYB transcription factor family by one-hybrid experiments in yeast. PLoS ONE *10*, e0141044.

Kieffer, M., Neve, J., and Kepinski, S. (2009). Defining auxin response contexts in plant development. Curr.Opin. Plant Biol. *13*, 12–20.

Kim, D.H., Yamaguchi, S., Lim, S., Oh, E., Park, J., Hanada, A., Kamiya, Y., and Choi, G. (2008). SOMNUS, a CCCH-type zinc finger protein in *Arabidopsis*, negatively regulates light-dependent seed germination downstream of PIL5. Plant Cell *20*, 1260–1277.

Lashbrooke, J., Cohen, H., Levy-Samocha, D., Tzfadia, O., Panizel, I., Zeisler, V., Massalha, H., Stern, A., Trainotti, L., Schreiber, L., et al. (2016). MYB107 and MYB9 homologs regulate suberin deposition in angiosperms. Plant Cell *28*, 2097–2116.

Lata, C., and Prasad, M. (2011). Role of DREB in regulation of abiotic stress response in plants. J. Exp. Bot. *62*, 4731–4748.

Lee, H.W., Kim, N.Y., Lee, D.J., and Kim, J. (2009). *LBD18/ASL20* regulates lateral root formation in combination with *LBD16/ASL18* downstream of *ARF7* and *ARF19* in Arabidopsis. Plant Physiol. *151*, 1377–1389.

Lim, S., Park, J., Lee, N., Jeong, J., Toh, S., Watanabe, A., Kim, J., Kang, H., Kim, D.H., Kawakami, N., et al. (2013). ABA-insensitive3, ABA-insensitive5, and DELLAs interact to activate the expression of SOMNUS and other high-temperature-inducible genes in *Arabidopsis*. Plant Cell *25*, 4863–4878.

Lin, J., Yu, L., and Xiang, C. (2019). ARABIDOPSIS NITRATE REGULATED 1 acts as a negative modulator of seed germination by activating *ABI3* expression. New Phytol. *225*, 835–847.

Liu, Y., Wang, R., Zhang, P., Chen, Q., Luo, Q., Zhu, Y., and Xu, J. (2016). The nitrification inhibitor methyl 3-(4-hydroxyphenyl)propionate modulates root development by interfering with auxin signaling via the NO/ROS pathway. Plant Physiol. *171*, 1686–1703.

Lopez-Molina, L., Mongrand, S., McLachlin, D.T., Chait, B.T., and Chua, N.-H. (2002). ABI5 acts downstream of ABI3 to execute an ABA-dependent growth arrest during germination. Plant J. *32*, 317–328.

Love, M.I., Huber, W., and Anders, S. (2014). Moderated estimation of fold change and dispersion for RNA-Seq data with DESeq2. Genome Biol. *15*, 550.

Mabuchi, K., Maki, H., Itaya, T., Suzuki, T., Nomoto, M., Sakaoka, S., Morikami, A., Higashiyama, T., Tada, Y., Busch, W., et al. (2018). MYB30 links ROS signaling, root cell elongation, and plant immune responses. Proc. Natl. Acad. Sci. U S A *115*, E4710–E4719.

Manzano, C., Pallero-Baena, M., Casimiro, I., De Rybel, B., Orman-Ligeza, B., Van Isterdael, G., Beeckman, T., Draye, X., Casero, P., and del Pozo, J.C. (2014). The emerging role of reactive oxygen species signaling during lateral root development. Plant Physiol. *165*, 1105–1119.

Mittler, R., Vanderauwera, S., Suzuki, N., Miller, G., Tognetti, V., Vandepoele, K., Gollery, M., Shulaev, V., and Van Breusegem, F. (2011). ROS signaling: the new wave? Trends Plant Sci. *16*, 1300–1309.

Mostofa, M., Ghosh, A., Li, Z.G., Siddiqui, M., Fujita, M., and Tran, L.S. (2018). Methylglyoxal – a signaling molecule in plant abiotic stress responses. Free Radic. Biol. Med. *122*, 96–109.

Naseer, S., Lee, Y., Catherine, L., Franke, R., Nawrath, C., and Geldner, N. (2012). Casparian strip diffusion barrier in *Arabidopsis* is made of a lignin polymer without suberin. Proc. Natl. Acad. Sci. U S A *109*, 10101–10106.

Okushima, Y., Fukaki, H., Onoda, M., Theologis, A., and Tasaka, M. (2007). ARF7 and ARF19 regulate lateral root formation via direct activation of *LBD/ASL* Genes in *Arabidopsis*. Plant Cell *19*, 118–130.

Park, J.E., Park, J.Y., Kim, Y.S., Staswick, P., Jeon, J., Yun, J., Kim, S., Kim, J., Lee, Y.H., and Park, C.M. (2007). GH3-mediated auxin homeostasis links growth regulation with stress adaptation response in *Arabidopsis*. J. Biol. Chem. *282*, 10036–10046.

Passardi, F., Cosio, C., Penel, C., and Dunand, C. (2005). Peroxidases have more functions than a Swiss army knife. Plant Cell Rep *24*, 255–265.

Passardi, F., Penel, C., and Dunand, C. (2004). Performing the paradoxical: how plant peroxidases modify the cell wall. Trends Plant Sci. *9*, 534–540.

Persak, H., and Pitzschke, A. (2014). Dominant repression by *Arabidopsis* transcription factor MYB44 causes oxidative damage and hypersensitivity to abiotic stress. Int. J. Mol. Sci. *15*, 2517–2537.

Pitzschke, A., Forzani, C., and Hirt, H. (2006). Reactive oxygen species signaling in plants. Antioxid.Redox Sign *8*, 1757–1764.

Reeves, W., Lynch, T., Mobin, R., and Finkelstein, R. (2011). Direct targets of the transcription factors ABA-Insensitive(ABI)4 and ABI5 reveal synergistic action by ABI4 and several bZIP ABA response factors. Plant Mol. Biol. *75*, 347–363.

Schreiber, L. (2010). Transport barriers made of cutin, suberin and associated waxes. Trends Plant Sci. *15*, 546–553.

Seo, K.I., Lee, J.H., Nezames, C., Zhong, S., Song, E., Byun, M.O., and Deng, X.W. (2014). ABD1 is an *Arabidopsis* DCAF substrate receptor for CUL4-DDB1-based E3 ligases that acts as a negative regulator of abscisic acid signaling. Plant Cell *26*, 695–711.

Seo, P.J., Xiang, F., Qiao, M., Park, J.Y., Lee, Y., Kim, S.G., Lee, Y.H., Park, W.J., and Park, C.M. (2009). The MYB96 transcription factor mediates

abscisic acid signaling during drought stress response in *Arabidopsis*. Plant Physiol. *151*, 275–289.

Shin, R., Burch, A., Huppert, K., Tiwari, S., Murphy, A., Guilfoyle, T., and Schachtman, D. (2007). The *Arabidopsis* transcription factor MYB77 modulates auxin signal transduction. Plant Cell *19*, 2440–2453.

Shu, K., Chen, Q., Wu, Y.R., Liu, R.J., Zhang, H.W., Wang, P.F., Li, Y.L., Wang, S.F., Tang, S.Y., Liu, C.Y., et al. (2016a). ABI4 mediates antagonistic effects of abscisic acid and gibberellins at transcript and protein levels. Plant J. *85*, 348–361.

Shu, K., Chen, Q., Wu, Y.R., Liu, R.J., Zhang, H.W., Wang, S.F., Tang, S.Y., Yang, W.Y., and Xie, Q. (2016b). ABSCISIC ACID-INSENSITIVE 4 negatively regulates flowering through directly promoting Arabidopsis *FLOWERING LOCUS C* transcription. J. Exp. Bot. *67*, 195–205.

Signora, L., Smet, I., Foyer, C.H., and Zhang, H. (2002). ABA plays a central role in mediating the regulatory effects of nitrate on root branching in *Arabidopsis*. Plant J. *28*, 655–662.

Staswick, P.E., Serban, B., Rowe, M., Tiryaki, I., Maldonado, M.T., Maldonado, M.C., and Suza, W. (2005). Characterization of an Arabidopsis enzyme family that conjugates amino acids to indole-3-acetic acid. Plant Cell *17*, 616–627.

Tiwari, S., Hagen, G., and Guilfoyle, T. (2003). The roles of auxin response factor domains in auxin-responsive transcription. Plant Cell *15*, 533–543.

Tsukagoshi, H., Busch, W., and Benfey, P. (2010). Transcriptional regulation of ROS controls transition from proliferation to differentiation in the root. Cell *143*, 606–616.

Tylová, E., Pecková, E., Blascheová, Z., and Soukup, A. (2017). Casparian bands and suberin lamellae in exodermis of lateral roots: an

important trait of roots system response to abiotic stress factors. Ann. Bot. *120*, 71–85.

Ulmasov, T., Murfett, J., Hagen, G., and Guilfoyle, T. (1997). Aux/IAA proteins repress expression of reporter genes containing natural and highly active synthetic auxin response elements. Plant Cell *9*, 1963–1971.

Vaahtera, L., Brosche, M., Wrzaczek, M., and Kangasjärvi, J. (2014). Specificity in ROS signaling and transcript signatures. Antioxid.Redox Sign *21*, 1422–1441.

Vanneste, S., and Friml, J. (2009). Auxin: a trigger for change in plant development. Cell *136*, 1005–1016.

Yadav, V., Molina, I., Ranathunge, K., Castillo, I.Q., Rothstein, S.J., and Reed, J.W. (2014). ABCG transporters are required for suberin and pollen wall extracellular barriers in *Arabidopsis*. Plant Cell *26*, 3569–3588.

Yang, Y., Zhang, L.B., Chen, P., Liang, T., Li, X., and Liu, H.T. (2019). UV-B photoreceptor UVR8 interacts with MYB73/MYB77 to regulate auxin responses and lateral root development. EMBO J. *39*, e101928.

Yu, Y., Wang, J., Li, S., Kakan, X., Zhou, Y., Miao, Y., Wang, F., Qin, H., and Huang, R. (2019). Ascorbic acid integrates the antagonistic modulation of ethylene and abscisic acid in the accumulation of reactive oxygen species. Plant Physiol. *179*, 1861–1875.

Yuan, H.-M., Xu, H., Liu, W.-C., and Lu, Y.-T. (2013). Copper regulates primary root elongation through PIN1-mediated auxin redistribution. Plant Cell Physiol *54*, 766–778.

Zhang, H.M., Aj, J., Barlow, P.W., and Forde, B.G. (1999). Dual pathways for regulation of root branching by nitrate. Proc. Natl. Acad. Sci. U S A *96*, 6529–6534.

Zhang, P., Wang, R.L., Ju, Q., Li, W.Q., Tran, L.S., and Xu, J. (2019a). The R2R3-MYB transcription factor MYB49 regulates cadmium accumulation. Plant Physiol. *180*, 529–542.

Zhang, X.X., Wang, X.Y., Zhuang, L.L., Gao, Y.L., and Huang, B.R. (2019b). Abscisic acid mediation of drought priming-enhanced heat tolerance in tall fescue (*Festuca arundinacea*) and *Arabidopsis*. Physiol. Plant. *167*, 488–501.

Zhao, X., Dou, L., Gong, Z., Wang, X., and Mao, T. (2018). BES1 hinders ABSCISIC ACID INSENSITIVE5 and promotes seed germination in *Arabidopsis*. New Phytol. *221*, 908–918.

Zhao, Y., Xing, L., Wang, X., Hou, Y.J., Gao, J., Wang, P., Duan, C.G., Zhu, X., and Zhu, J.K. (2014). The ABA receptor PYL8 promotes lateral root growth by enhancing MYB77-dependent transcription of auxin-responsive genes. Sci. Signal. *7*, ra53.

Zheng, Y., Schumaker, K., and Guo, Y. (2012). Sumoylation of transcription factor MYB30 by the small ubiquitin-like modifier E3 ligase SIZ1 mediates abscisic acid response in *Arabidopsis thaliana*. Proc. Natl. Acad. Sci. U S A *109*, 12822–12827.

Zhou, X., Hao, H., Zhang, Y., Bai, Y., Zhu, W., Qin, Y., Yuan, F.F., Zhao, F., Wang, M., Hu, J., et al. (2015). SOS2-LIKE PROTEIN KINASE5, an SNF1-RELATED PROTEIN KINASE3-Type protein kinase, is important for abscisic acid responses in arabidopsis through phosphorylation of ABSCISIC ACID-INSENSITIVE5. Plant Physiol. *168*, 659–676.

Zhou, Y.B., Liu, C., Tang, D.Y., Yan, L., Wang, D., Yang, Y.Z., Gui, J., Zhao, X.Y., Li, L.G., Tang, X.D., et al. (2018). The receptor-like cytoplasmic kinase STRK1 phosphorylates and activates CatC, thereby regulating H_2O_2 homeostasis and improving salt tolerance in rice. Plant Cell *30*, 1100–1118.

STAR★METHODS

KEY RESOURCES TABLE

REAGENT or RESOURCE	SOURCE	IDENTIFIER
Antibodies		
Anti-HA tag antibody	Abcam	CAT#AB13834; RRID:AB_443010
Anti-Myc tag antibody	Abcam	CAT#AB172; RRID:AB_302595
Anti-His tag antibody	Abcam	CAT#AB14923; RRID:AB_443105
Anti-GST tag antibody	Abcam	CAT#AB19256; RRID:AB_444809)
Anti-ABI5 antibody	Abcam	CAT#AB98831; RRID:AB_10670685
Anti-GFP tag antibody	Abcam	CAT#AB13970; RRID:AB_300798
Anti-RPN6 antibody	Enzo	CAT#BML-PW8370; RRID:AB_10541615
HRP-Goat anti-Rabbit IgG (H+L) secondary antibody	Thermo	CAT#31460; RRID:AB_228341
Bacterial and virus strains		
Agrobacterium tumefaciens GV3101	Zhang et al., 2019a	N/A
Rosetta (DE3) chemically competent cells	Zhang et al., 2019a	CAT#J43270
Biological samples		
Y2HGold chemically competent cells	Clontech	N/A
Yeast strain AH109	Clontech	N/A
Chemicals, peptides, and recombinant proteins		
Sudan black B	BBI	CAT#A602008
Fluorescein diacetate	BBI	CAT#A600202
3,3'-diaminobenzidine	BBI	CAT#A690009
Fluorol Yellow 088	MKBio	CAT#MX4473
BES-H_2O_2-Ac	WAKO	CAT#028-17811
Isopropyl-β-D-thiogalactopyranoside	WAKO	CAT#090-05141
Ni-NTA agarose	Qiagen	CAT#30210
Dihydroethidium	Beyotime	CAT#S0063
2-(4-Amidinophenyl)-6-indolecarbamidine dihydrochloride	Beyotime	CAT#C1005
Propidium Iodide	Beyotime	CAT#ST511
3-indoleacetic acid	Sigma-Aldrich	CAT#I2886
Abscisic acid	Sigma-Aldrich	CAT#90769
MG132, a proteasome inhibitor	Sigma-Aldrich	CAT#M7449
Cycloheximide, a protein synthesis inhibitor	Sigma-Aldrich	CAT#C7698
AtMYB70-His	This study	N/A
GST-ABI5	This study	N/A
AtMYB70-HA	This study	N/A
AtABI5-HA	This study	N/A
Critical commercial assays		
Glutathione HiCap Matrix	Qiagen	CAT#30900
Dual-Luciferase® Reporter Assay System	Promega	CAT#E1910
RNAiso Plus Kit	Takara	CAT#9109
PrimeScriptTM RT reagent Kit with gDNA Eraser	Takara	CAT#RR047A

Continued

REAGENT or RESOURCE	SOURCE	IDENTIFIER
UltraSYBR Mixture	CWBIO	CAT#CW0957M
Matchmaker® Gold Yeast One-Hybrid Library Screening System	Clontech	CAT#630491
Matchmaker™ Gold Yeast Two-Hybrid System	Clontech	CAT#630489
Clarity Western ECL Substrate	Bio-Rad	CAT#1705060
SurePAGE™, Bis-Tris, 10x8, 4-20%	Genscript	CAT#M00656
Tris-MOPS-SDS Running Buffer Powder	Genscript	CAT#M00138
Tanon™ High-sig ECL Western Blotting Substrate	Tanon	CAT#180-501
Developer and Fixer Kit for Black and White Film and Paper	Beyotime	CAT#P0019
SDS Lysis Buffer	Beyotime	CAT#P0013G
LightShift Chemiluminescent EMSA Kit	Beyotime	CAT#GS009
Deposited data		
Raw RNA sequencing data	This study	NCBI Sequence Read Archive: PRJNA056033
Experimental models: organisms/strains		
Arabidopsis: myb70-1	NASC	SALK_208583
Arabidopsis: myb70-2	NASC	GK_350C10
Arabidopsis: abi5-8	Zheng et al., 2012	SALK_013163
Arabidopsis: ABI5OX	Bu et al., 2009	Transgenic Col-0
Arabidopsis: DR5:GUS	Ulmasov et al., 1997	Transgenic Col-0
Arabidopsis: DR5:GFP	Friml et al., 2003	Transgenic Col-0
Arabidopsis: upb1	Tsukagoshi et al., 2010	SALK_115536
Arabidopsis: 35S::UPB1-3YFP	Tsukagoshi et al., 2010	Transgenic Col-0
Arabidopsis: MYB70OX-1	This study	Transgenic Col-0
Arabidopsis: MYB70OX-2	This study	Transgenic Col-0
Arabidopsis: MYB70OX-3	This study	Transgenic Col-0
Arabidopsis: MYB70OX-4	This study	Transgenic Col-0
Arabidopsis: MYB70OX-5	This study	Transgenic Col-0
Arabidopsis: MYB70OX-6	This study	Transgenic Col-0
Arabidopsis: proMYB70:GUS	This study	Transgenic Col-0
Arabidopsis: proMYB70:MYB70-GFP	This study	Transgenic Col-0
Arabidopsis: myb70-1/DR5:GFP	This study	Cross between DR5:GFP and myb70-1
Arabidopsis: MYB70OX-3/DR5:GFP	This study	Cross between DR5:GFP and MYB70OX-3
Arabidopsis: myb70-1/DR5:GUS	This study	Cross between DR5:GUS and myb70-1
Arabidopsis: MYB70OX-3/DR5:GUS	This study	Cross between DR5:GUS and MYB70OX-3
Arabidopsis: myb70-2/abi5-8	This study	Cross between myb70-2 and abi5-8
Arabidopsis: myb70-2/ABI5OX	This study	Cross between myb70-2 and ABI5OX
Arabidopsis: MYB70OX-3/abi5-8	This study	Cross between MYB70OX3 and abi5-8
Arabidopsis: MYB700X-3/ABI5OX	This study	Cross between MYB70OX3 and ABI5OX
Tobacco: Nicotiana benthamiana	This study	N/A
Oligonucleotides		
Primers used are shown in Table S1	This study	N/A

(Continued on next page)

Continued		
REAGENT or RESOURCE	SOURCE	IDENTIFIER
Recombinant DNA		
pGreen II 62-AtABI5	This study	N/A
pGreen II 62-AtMYB70	This study	N/A
pGreenII 0800-AtEM1	This study	N/A
pGreenII 0800-AtEM6	This study	N/A
pGreenII 0800-AtGH3.3	This study	N/A
pGreenII 0800-AtPER57	This study	N/A
pGreenII 0800-AtGPAT5	This study	N/A
pGAL4-AtMYB70-N	This study	N/A
pGAL4-AtMYB70-C	This study	N/A
pGAL4-AtMYB70-C(ΔEAR)	This study	N/A
pGAL4-VP16	This study	N/A
pGAL4-VP16-AtMYB70	This study	N/A
pGBKT7-AtABI5	This study	N/A
pGADT7-AtMYB70	This study	N/A
pET30a-AtMYB70	This study	N/A
pGEX4T-1-AtABI5	This study	N/A
pCN173-AtABI5	This study	N/A
pYN173-AtMYB70	This study	N/A
pYN173-AtMYB70	This study	N/A
Software and algorithms		
IBM SPSS Statistics	Statistical Analysis System	https://www.ibm.com/analytics/spss-statistics-software
ImageJ	NIH, USA	https://imagej.nih.gov/ij/
DESeq2	Love et al., 2014	http://www.bioconductor.org/packages/release/bioc/html/DESeq2.html

RESOURCE AVAILABILITY

Lead contact

Further information and requests for resources should be directed to and will be fulfilled by the lead contact, Jin Xu (xujin@sxau.edu.cn; xujinsxau@163.com).

Materials availability

All materials generated in this study are available from the lead contact without restriction. This study did not generate new unique reagents.

Data and code availability

Raw RNA sequencing data derived from *A. thaliana* samples have been deposited in the Short Read Archive database of NCBI, and accession number PRJNA506033 is listed in the key resources table.

This paper does not report original code.

Any additional information required to reanalyze the data reported in this paper is available from the lead contact upon request.

EXPERIMENTAL MODEL AND SUBJECT DETAILS

Arabidopsis thaliana

Plants of the Columbia-0 (Col-0) wild-type genetic background and mutants were used in this study. Mutant *myb70-1* (SALK_208583) and *myb70-2* (GK_350C10) seeds were obtained from the European Arabidopsis Stock Centre (NASC). The *upb1* and *35S::UPB1-3YFP* (Tsukagoshi et al., 2010) mutant was kindly donated by Professor Philip N. Benfey (Duke University). The previously described T-DNA insertion *abi5* mutant designated *abi5-8* (SALK_013163) was used (Zheng et al., 2012). *myb70/abi5-8*, *MYB70OX/abi5-8*, *myb70/ABI5-OX*, *MYB70OX/ABI5OX*, *myb70-1/DR5:GUS*, *MYB70OX-3/DR5:GUS*, *myb70-1/DR5:GFP*, and *MYB70OX-3/DR5:GFP* double mutants were acquired by crossing *myb70* or *MYB70OX3* with *abi5-8* or ABI5OX (Bu et al., 2009) lines, *myb70-1* or *MYB70OX-3* with *DR5:GUS* (Ulmasov et al., 1997) or *DR5:GFP* (Friml et al., 2003) lines, respectively, and confirmed by PCR.

Arabidopsis seeds were surface-sterilized using 50% bleach (v/v), rinsed with sterile water five times, and sown on 1/2-strength MS medium comprising 1% sucrose (w/v) and 0.65% or 1% agar (w/v), with the pH adjusted to 5.75 via 1 M KOH or 3% HCl. The agar plates were stratified at 4°C for 2 days before being transferred to a growth chamber maintained at 22°C under a 16-h-light/8-h-dark photoperiod. Five-day-old seedlings were transplanted onto fresh agar medium that contained different chemicals for various indicated times.

Bacterial strains

Agrobacterium tumefaciens GV3101 was cultivated in Luria-Bertani (LB) medium supplemented with appropriate antibiotic in a shaker at 28°C; Rosetta (DE3) chemically competent cells was cultivated in LB medium supplemented with appropriate antibiotic in a shaker at 37°C.

METHOD DETAILS

Phenotypic analysis

After the seedlings were treated for the indicated time, images were taken by using an Epson Perfection V500 Photo scanner (Japan), after which the PR length, LR number and LR density were determined using ImageJ (v1.52a). With respect to LRP initiation, four stages were quantified (Zhang et al., 1999). For root MZ and EZ length analyses were determined (Casamitjana-Martınez et al., 2003; Yuan et al., 2013), the seedlings treated for the indicated times were mounted in 1 μg mL^{-1} propidium iodide (PI) staining solution, after which images were taken by an LSM 710 confocal laser scanning microscope (Carl Zeiss, Germany). The lengths were subsequently determined using ImageJ.

Plasmid construction and transformation

The full-length *MYB70* coding region was amplified from *Arabidopsis* cDNA, and *MYB70* overexpression lines were subsequently generated by inserting *MYB70* PCR products into a pCAMBIA1300 vector harboring the CaMV *35S* promoter. To generate *proMYB70:GUS* constructs the 1.5-kb promoter sequence upstream of the ATG start codon of the *MYB70* gene of *Arabidopsis* genomic DNA was amplified by gMYB70-forward (gMYB70-F) and gMYB70-reverse (gMYB70-R) primers and then inserted into a pCAMBIA1381 expression vector. With respect to the *proMYB70:MYB70-GFP* lines, the same primers were used to amplify the promoter containing a 1.5-kb sequence containing the *MYB70* gene coding region from *Arabidopsis* genomic DNA, which was subsequently introduced into a pCAMBIA1302 vector. Through the Agrobacterium-mediated floral dip method, the above constructs were transformed into Col-0 to generate transgenic *Arabidopsis* materials.

Seed germination analysis

For seed germination rate analysis, sterilized seeds were stratified at 4°C for 2 days and then sown on 1/2-strength MS medium consisting of 0, 0.5 or 1 μM ABA. The numbers of seed radicle appearance were determined at indicated times.

qRT-PCR and transcriptome analyses

Col-0, *myb70* mutant and *OX70* seedlings grown in 1/2-strength MS medium for 5 days and then transplanted to fresh medium supplemented with 10 μM ABA or 10 μM IAA for 0, 12 and 24 h. Total RNA was isolated using RNAiso Plus (TaKaRa, Dalian, China). After the RNA concentration was determined, reverse

transcription was performed using a PrimeScript™ RT Reagent Kit in conjunction with gDNA Eraser (TaKaRa) and oligo (dT) 18 primers. qRT-PCR analyses were performed using 2× UltraSYBR mixture (CWBIO, Beijing, China) on a LightCycler 480II platform (Roche, Switzerland). *ACTIN8* was used as an internal control (Liu et al., 2016). A DNA melting curve with only one peak for the specific primers used was used in conjunction with qRT-PCR, and all tested genes were subjected to three technical repetitions and included three independent biological replications.

For transcriptome analyses, total RNA was extracted from 5-day-old *Arabidopsis* Col-0, *myb70-2* mutant and *MYB70X-3* seedlings using RNAiso Plus (TaKaRa), and cDNA was synthesized using a PrimeScript™ RT Reagent Kit in conjunction with gDNA Eraser (TaKaRa). The mRNA was purified by oligo (dT) magnetic bead adsorption and was fragmented randomly using fragmentation buffer. First- and second-stranded cDNAs were subsequently synthesized with 6-bp random hexamers as primers. The cDNA was then purified with AMPure XP beads, followed by end repair and the addition of an A tail. The cDNA was then linked to the sequencing adaptor and subjected to fragment size selection via AMPure XP beads. After PCR amplification and thermal denaturation of their products into single strand, a single-stranded circular DNA library was obtained by cycling the single-stranded DNA with a bridge primer. Comparative transcriptome analysis was performed using the BGISEQ-500 platform (BGI, Wuhan, China). The RNA sequencing data have been archived in the Short Read Archive database of the National Center for Biotechnology Information under the accession No. PRJNA506033. The RNA-seq data were trimmed using Trimmomatic (v0.36) program and mapped against *A. thaliana* annotated genes (TAIR10_Araport11) using Bowtie2 (v2.2.5). Gene expression levels were then calculated using RSEM (v1.2.8) program. DEGs were identified by a $\log_2$ fold change ≥ 1 or ≤ -1 and $q \leq 0.001$ thresholds using DESeq2 (Love et al., 2014).

In vitro pull-down, Y1H, and Y2H assays

In vitro pull-down assays, full-length coding DNA sequences (CDSs) of *MYB70* and *ABI5* were cloned into pET30a and pGEX4T-1 expression vectors, respectively. After induction by 0.1 mM isopropyl-β-D-thiogalactopyranoside (IPTG), the expression vector fused into Rosetta (DE3) chemically competent cells, and MYB70-His and GST-ABI5 proteins were expressed. Soluble GST or GST-ABI5 recombinant proteins were isolated and fixed by the glutathione HiCap matrix (Qiagen GmbH, Hilden, Germany). Using the fixed GST or GST-ABI5 proteins to incubate the MYB70-His protein, the interaction with anti-His antibodies (Sigma-Aldrich) was detected by western blot analysis. The details of the primers used are presented in Table S1.

Y1H assays were conducted using a Matchmaker Gold Yeast One-Hybrid Library Screening System (Clontech). The amplified promoter fragments of MYB70 target genes were fused into a pAbAi vector to generate pBait-AbAi constructs. The constructs were then transferred into the yeast strain Y1HGold and subsequently selected. The coding regions of *MYB70* were amplified from *A. thaliana* genomic DNA, ligated to the a pGADT7 prey vector to generate AD-MYB70, introduced into the strain Y1HGold pBait-AbAi, and subsequently selected on synthetic dropout (SD)/-Leu/aureobasidin A (AbA) medium. The primers used are listed in Table S1.

The Y2H assays were conducted in accordance with the Matchmaker manufacturer's protocol (Clontech, USA). The pGBKT7 (BD) bait plasmid vector was used to introduce the full-length CDSs of *ABI5* and *UPB1*, respectively, and a pGADT7 (AD) prey vector was used to clone the full-length CDS of *MYB70*. The constructs were then inserted into yeast strain Y2HGold cells. SD/-Leu/-His/-Ade/-Trp medium (Clontech, USA) supplemented with 40 μg mL^{-1}5-bromo-4-chloro-3-indolyl-α-D-galactopyranoside (X-α-Gal) was used to select yeast transformants that were grown at 30°C for approximately 3 days, and afterward, the potential interactions between proteins were determined. The primers used are listed in Table S1.

Co-IP analysis

The full-length CDSs of *MYB70* and *ABI5* were amplified and then fused into tagging vectors with HA or Myc tags, respectively, harboring the CaMV 35S promoter. Next, transient expression mediated by agroinfiltration in *N. benthamiana* leaves was performed. The total protein extractions were used to immunoprecipitate with anti-HA antibodies, after which anti-Myc antibodies were used to coimmunoprecipitate ABI5-Myc. The specific primers used are presented in Table S1.

ChIP assays

For ChIP assays, approximately 2.5 g of *proMYB70:MYB70-GFP* seedlings were thoroughly rinsed with distilled water, after which they were flash frozen and finely ground with a mortar and pestle. Next, the chromatin DNA of the samples was isolated and subjected to ultrasonic interruptions, after which it was incubated in ChIP dilution buffer consisting of chromatin solution and protein G-agarose beads (Upstate Biotechnology, Lake Placid, NY). Anti-GFP (ab290, Abcam, Cambridge, United Kingdom) was used to immunoprecipitate the protein-DNA complex by incubating and gently rotating the mixture at 4°C overnight. After the samples were eluted and DNA purification, qRT-PCR was then conducted for GFP-specific enrichment of the fragments from the promoters of the *GH3.3*, *PER57* and *GPAT5* genes. The primers used are listed in Table S1.

BiFC assay

A pCAMBIA1300 vector was used to clone the amplified full-length CDSs of *MYB70* and *ABI5* and to construct C-terminal in-frame recombinants with C-YFP and N-terminal in-frame recombinants with N173 YFP. The generated plasmids were introduced into *A. tumefaciens* strain GV3101 (pSoup-p19), which were then coinjected into *N. benthamiana* leaves for approximately 72 h. The fluorescence in epidermal cells stained with 4′,6-diamidino-2-phenylindole (DAPI) was examined via an LSM 710 microscope (Carl Zeiss, Germany). Three independent experiments were carried out, five plants were used, and more than ten leaves were infected for each independent experiment. The primers used are presented in Table S1.

Immunoblotting analysis

Seeds of wild-type Col-0 and *OX70-3*, which were grown in the same growth chamber and harvested at the same day, were sown on MS medium containing 5 μM ABA and cultivated in a growth chamber under continuous white light for 3 d. After being washed twice with liquid MS medium, the seeds were transferred to fresh liquid MS medium supplemented with or without 50 μM MG132 (Sigma-Aldrich) or 100 μM CHX (Sigma-Aldrich), and harvested at the indicated time points. Subsequently, total proteins were extracted from the samples using SDS lysis buffer (Beyotime) and accurately quantified. After mixing with 5 × SDS-loading buffer, the proteins were boiled for 10 min, isolated on a 10% SDS-PAGE gel, and subsequently transferred to polyvinylidene fluoride (PVDF) membrane and incubated in blocking buffer (20mM Tris-HCl, 150 mM NaCl, 0.05% Tween 20, 5% nonfat milk powder) for 1 h at room temperature, then with 1:2000 anti-ABI5 (Abcam) or 1:1,000 anti-RPN6 (Enzo) for 12 h at 4°C, and followed with HRP-conjugated goat anti-rabbit IgG (Thermo) for 1 h. Finally, the PVDF membrane was overlaid on high-sig ECL western blotting substrate (Tanon) for 5 min and imaged using a CHEMI DOC^{TM}XRS (Bio-rad).

Dual-luciferase (LUC) reporter assays

The full-length *ABI5* and *MYB70* coding regions were amplified and then transferred into a pGreen II 62-SK vector, after which pGreenII 0800-LUC double-reporter vector was fused to the promoter fragments of *EM1* (2070 bp) and *EM6* (1,364 bp). The above constructs were then transferred into *A. tumefaciens* strain GV3101 (pSoup-p19), and *pro35S:MYB70*, *pro35S:ABI5*, *proEM1:LUC* and *proEM6:LUC* recombinant strains were generated. The *pro35S:MYB70* and/or *pro35S:ABI5* with *proEM1:LUC* as well as the *pro35S:MYB70* and/or *pro35S:ABI5* with *proEM6:LUC* strains were subsequently coinfiltrated into *N. benthamiana* leaves and cultivated for 3 days in a growth chamber supplemented in the presence or absence of 5 μM ABA; *proEM1:LUC* or *proEM6:LUC* was used as an internal control. The promoters of *GH3.3* (1,556 bp), *PER57* (1,443 bp) and *GPAT5* (1,559 bp) were amplified and cloned into pGreenII 0800-LUC. The constructs were transferred into *A. tumefaciens* strain GV3101 (pSoup-p19), and *proGH3.3:LUC*, *proPER57:LUC* and *proGPAT5:LUC* recombinant strains were generated. The *pro35S:MYB70* with *proGH3.3:LUC* or *proPER57:LUC* or *proGPAT5:LUC* were subsequently coinfiltrated into *N. benthamiana* leaves (TF-encoding gene fused to *35S* promoter/promoter-LUC fusions in pGreenII 0800-LUC ratio = 9/1, v:v) (Hellens et al., 2005) and cultivated for 72 h in a growth chamber supplemented in the presence or absence of 5 μM ABA or 0.5 μM IAA.

For the transcriptional activity analyses of MYB70, the full-length *MYB70* coding region and the truncated MYB70 fragments, including the MYB70-C (628 to end, containing EAR motif), the EAR motif containing region (628–673), the MYB70-N (1–627) and the truncated MYB70-C without EAR motif (673 to end), were PCR amplified and were then fused to the GAL4 DNA binding domain (BD), driven by the 35S promoter,

respectively. VP16 is a transcriptional activator that was used as a positive control and GAL4-BD was used as a negative control. These constructs were transferred into *A. tumefaciens* strain GV3101 (pSoup-p19), respectively, and then transiently expressed in *N. benthamiana* leaves.

After inoculation and a transient incubation of 72 h, a dual-LUC reporter assay system (Promega), which included firefly LUC and *Renilla* (REN) LUC, was used to measure the relative LUC activity. Two cm^2 leaf discs were sampled and fine-ground in 500 μL of Passive Lysis Buffer, and then 8 μL of rude extract were added to 40 μL of Luciferase Assay Buffer (Hellens et al., 2005). Finally, the activity of the promoter was determined by the LUC/REN value using a luminometer (Modulus™, Promega). Three independent biological experiments were conducted. The specific primers used are listed in Table S1.

Electrophoretic mobility shift assay. Electrophoretic mobility shift assay (EMSA) was conducted using a LightShift Chemiluminescent EMSA Kit (GS009, Beyotime, China) according to Zhang et al. (2019a). After induction by IPTG, MYB70·His and GST·ABI5 proteins were purified by Ni-NTA agarose (Qiagen) and a glutathione HiCap matrix, respectively. The wild-type and mutant probe sequences used are listed in Table S1.

Quantification of endogenous ABA and IAA level

Five-day-old *Arabidopsis* seedlings were used for the quantification of IAA and ABA. Approximately 0.5 g (fresh weight) samples were collected and frozen in liquid nitrogen. The frozen tissues were finely ground with a mortar and pestle and extracted using 80% acetone, and the crude extracts were purified by a sequence of steps, including filtration and partitioning, followed by methylation by a diazomethane gas stream and resuspension in 100 mL of ethyl acetate. The endogenous ABA and IAA levels were ultimately detected separately by GC-MS (5975C-7890A, Agilent Technologies, USA).

Fluorescence microscopy

For GFP visualization, 5-day-old *DR5:GFP*, *myb70b-1/DR5:GFP*, *MYB70OX/DR5:GFP* and *35S:MYB70-GFP* marker lines were subjected to confocal laser microscopy (LSM 710, Carl Zeiss, Germany) at an excitation wavelength of 488 nm and an emission wavelength of 509 nm.

Penetration assay

The apoplastic tracers PI and FDA were used to measure root uptake ability (Cohen et al., 2020). In brief, 9-day-old seedlings exhibiting three different phenotypes were incubated in 10 mg mL^{-1} FDA solution for 30 s in the dark and subsequently counterstained with 50 mg mL^{-1} PI solution. The FDA and PI fluorescences were then immediately captured for 2–10 min at 4-min intervals using an LSM 710 confocal microscope (Carl Zeiss, Germany).

Histological analysis

For GUS staining analysis, *proMYB70:GUS* seeds and seedlings at different developmental stages , 9-day-old *DR5:GUS*, *myb70-1/DR5:GUS,* and *MYB70OX/DR5:GUS* were used. The samples were immersed in GUS staining solution consisting of 1 mM 5-bromo-4-chloro-3-indolyl-b-D-GlcA cyclohexyl-ammonium (Sigma-Aldrich) for 1 h at 37°C. After the samples were washed and placed in 75% (w/v) ethanol, a Carl Zeiss imaging system (Axio Imager A2/HM525 NX UV) was used to collect images.

For *in vivo* ROS detection, the O_2^--specific probe DHE and the H_2O_2 probe BES-H_2O_2-Ac were used to examine O_2^- and H_2O_2, respectively. The seedlings were incubated in 10 μM DHE or 50 μM BES-H_2O_2-Ac for 1 h at 37°C in the dark, rinsed briefly in water, and then imaged using an LSM 710 instrument. To detect H_2O_2 using DAB staining, the seedlings were immersed in a 1 mg mL^{-1} solution for 3 h, washed five times and then imaged.

To analyze the lipid polyesters in the roots, Sudan black staining was performed. The roots were incubated in a solution consisting of 1% (w/v) Sudan black in 75% ethanol for 1 h. After rinsed with water, the roots were imaged.

For suberin lamella analysis, FY staining was conducted. Suberin lamellae of 9-day-old *Arabidopsis* roots were examined. After staining with a solution consisting of 0.01% fluorol yellow 088 (w/v, lactic acid) for

30 min at 70°C in the dark, the samples were gently rinsed with water and then imaged using an LSM 710 instrument.

Root suberin chemical composition analysis

The roots of 9-day-old seedlings grown 1/2-strength MS medium were harvested for suberin analysis. After a sequence of tissue delipidation and depolymerization, the samples were derivatized for free hydroxyl and carboxyl groups. Subsequently, 100 μL pyridine and 100 μL acetic anhydride were added to the methylation tube followed by cooling and evaporating under nitrogen gas. Finally, the samples were redissolved in 100 μL heptane:toluene (1:1 v:v) and the aliphatic suberin composition was determined using gas chromatography flame ionization detection (GC-FID).

Metal element content analysis

Nine-day-old seedlings were transplanted to 1/2-strength MS liquid medium for 3 weeks, at which point their roots and leaves were harvested. 1 mM EDTA solutions were used to chelate surface ions of the harvested tissues for 30 min, after which the samples were fixed in an oven at 105°C for 1 h and then oven-dried at 70°C until they reached a constant weight. Concentrated nitric acid was subsequently used to wet wash the samples for 72 h followed by boiling for 2 h. Finally, the following mineral elements were quantified by using inductively coupled plasma atomic emission spectroscopy (ICP-AES; iCAP6300, Thermo Fisher Scientific, Waltham, MA, USA): K, calcium (Ca), Fe, Mn, zinc (Zn) and Cu. Each experiment was repeated three times.

Accession numbers

The sequence data for genes analyzed in this study could be found in *Arabidopsis* Genome Initiative as followings: At2g36270 (*ABI5*), At1g49240 (*ACTIN8*), At3g51810 (*EM1*), At2g40170 (*EM6*), At5g63560 (*FACT*), At5g58860 (*CYP86A1*), At5g23190 (*CYP86B1*), At2g14960 (*GH3.1*), At2g23170 (*GH3.3*), At4g27260 (*GH3.5*), At3g11430 (*GPAT5*), At5g06090 (*GPAT7*), At2g23290 (*MYB70*), At1g05250 (*PER2*), At1g30870 (*PER7*), At1g34510 (*PER8*), At1g68850 (*PER11*), At2g35380 (*PER20*), At3g49120 (*PER34*), At5g14130 (*PER55*), At5g17820 (*PER57*), At5g47000 (*PER65*), At5g12420 (*WSD7*) and At2g47270 (*UPB1*).

QUANTIFICATION AND STATISTICAL ANALYSIS

All the details of the statistics presented in this study are provided in the Method Details section. Student's *t* test or one-way analysis of variance (ANOVA) followed by Tukey's test were performed in IBM SPSS Statistics v20 software, together with asterisk symbols (*) and different lowercases were shown as significant difference at $p < 0.05$, respectively.